

Received November 29, 2020, accepted December 13, 2020, date of publication December 24, 2020, date of current version January 5, 2021.

Digital Object Identifier 10.1109/ACCESS.2020.3047193

# Reverse-Order Multi-Objective Evolution Algorithm for Multi-Objective Observer-Based Fault-Tolerant Control of T-S Fuzzy Systems

BOR-SEN CHEN<sup>1,2</sup>, (Life Fellow, IEEE), MIN-YEN LEE<sup>1</sup>, WEI-YU CHEN<sup>3</sup>,  
AND WEIHAI ZHANG<sup>4</sup>, (Senior Member, IEEE)

<sup>1</sup>Department of Electrical Engineering, National Tsing Hua University, Hsinchu 30013, Taiwan

<sup>2</sup>Department of Electrical Engineering, Yuan Ze University, Chung-Li 32003, Taiwan

<sup>3</sup>Research Center for Information Technology Innovation (CITI), Academia Sinica, Taipei 115, Taiwan

<sup>4</sup>College of Electrical Engineering and Automation, Shandong University of Science and Technology, Qingdao 266590, China

Corresponding author: Bor-Sen Chen (bschen@ee.nthu.edu.tw)


This work was supported by the Ministry of Science and Technology of Taiwan under Grant MOST 108-2221-E-007-099-MY3.

**ABSTRACT** In this study, a multi-objective  $H_2/H_\infty$  observer-based fault-tolerant control (FTC) design with reverse-order multi-objective evolution algorithm (MOEA) is proposed to deal with the FTC problem of Takagi-Sugeno (T-S) fuzzy systems. To achieve the optimal robust FTC design for the T-S fuzzy systems under the sensor and actuator faults, as well as external disturbance and measurement noise, the multi-objective  $H_2/H_\infty$  observer-based FTC scheme is proposed to efficiently estimate the system state and the fault signals based on a proposed smoothed fault signal model. Then, multi-objective  $H_2/H_\infty$  FTC performance can be achieved by an estimated state and fault signal feedback scheme to efficiently compensate the effect of fault signals and attenuate the effect of external disturbance. By using the proposed indirect method, the multi-objective  $H_2/H_\infty$  observer-based FTC design problem is transformed into linear matrix inequalities (LMIs)-constrained multi-objective optimization problem (MOP). Besides, to overcome the difficulties in searching large fuzzy parameters of observer-based FTC design for solving the LMIs-constrained MOP, a reverse-order MOEA is proposed to overcome the bottleneck to efficiently solve the MOP for multi-objective  $H_2/H_\infty$  observer-based FTC of T-S fuzzy system by searching feasible objective vectors in the objective space instead of searching fuzzy design parameters in the parametric space. Two practical examples are considered for the performance validation with (i)  $H_2/H_\infty$  observer-based FTC design for the missile guidance system with the actuator and sensor fault signals due to the sudden cheating side-step maneuvering and the hostile jamming interference and (ii)  $H_2/H_\infty$  observer-based FTC design for inverted pendulum system which effected by the constant actuator fault.

**INDEX TERMS** Reverse-order multi-objective evolution algorithm (MOEA), Takagi-Sugeno (T-S) fuzzy systems, multi-objective problems (MOP), observer-based fault tolerant control, missile guidance system, actuator and sensor fault.

## I. INTRODUCTION

Along with the development of modern industrial production, due to the fact that the actuator and sensor in the control system become much vulnerable to the fault signal, higher requirements of safety and reliability for the control plant have put forward. In order to ensure safety and reliability in the industrial process, the capability of fault tolerance during the control process has become an important issue and caught

The associate editor coordinating the review of this manuscript and approving it for publication was Radu-Emil Precup .

the sight of control engineers. In the case of passive fault-tolerant control (FTC) design, which considers the fault as a specific external disturbance, it aims to achieve the control performance with a prescribed fault tolerance level [1]–[3]. On the other hand, for the active FTC scheme, the fault signals are estimated by an observer and the estimated faults will be used to eliminate the effect of real faults. The FTC techniques have been widely investigated and applied in several fields. To attenuate the high-frequency variation effect from the actuator, the FTC is applied for attitude control of the satellite in [4]. In [5], the FTC control was used to stabilize the linear

quantum system with the consideration of random voltage fluctuations. In [6], the operator theory-based fault-tolerant control was applied to MIMO microreactor. Also, in [7], a fault-tolerant control was developed for hypersonic flight vehicle with the multiple sensor faults.

For almost the physical systems, there has strongly non-linearity behavior in the physical system. Also, most fault signals are the nonlinear functions, which are coupled with state variables and control inputs in the physical system. While considering the effect of faults in the nonlinear system, the nonlinear fault functions will increase the difficulty of FTC analysis [6]–[8]. In recent years, the Takagi-Sugeno (T-S) fuzzy model has been considered as an efficient tool to describe the nonlinear dynamic systems [9], [10]. By utilizing the T-S fuzzy approximation method, the nonlinear system can be approximated by interpolating a set of local linear systems and the control design for the nonlinear system can be simplified by a set of fuzzy controllers. The T-S fuzzy model based control scheme has been widely investigated in several control issues [11]–[14]. Moreover, the fuzzy adaptive FTC scheme has been proposed for the fault-tolerant tracking control of a class of uncertain nonlinear systems with the non-affine nonlinear faults [15]. A back-stepping fuzzy control scheme is proposed to deal with the stabilization problem with the consideration of actuator faults in [16]. In [17], the event-triggered FTC design for network-based fuzzy systems is also discussed.

In general, the environmental noise is inevitable during the control process. Thus, it is expected that the FTC design can not only achieve the great FTC performance while the system is affected by the fault but also achieve some prescribed robust control performance for the disturbance attenuation. For this reason, several mixed FTC designs such as mixed optimal FTC control schemes [18], [19] and mixed robust FTC control schemes [20], [21] are developed. By extending the concept of mixed control method [22], [23], the multi-objective (MO) design has become a popular issue and addressed in many research topics on control and estimation [24]–[29]. Compared with the conventional mixed  $H_2/H_\infty$  control design schemes [22], [23] which have an unique optimal control strategy, there exist several optimal control strategies with the corresponding multi-objective optimal performance in a multi-objective control design. Based on the MO control design, the engineers are free to choose the preferred control strategy from the several optimal control strategies according to their own demands. To the best of authors' knowledge, there have very few studies to address the fuzzy MO FTC problem of nonlinear systems under sensor and actuator faults. Further, in the conventional FTC designs, the descriptor observer is always employed for fault signal estimation [16]–[21]. Since the augmented descriptor observer system is singular, more effort is needed for the robust FTC design. Therefore, the conventional FTC schemes are not suitable for MO FTC. In this study, a smoothed dynamic model is proposed to efficiently describe the actuator and

sensor fault signals. Since the augmented system with fault dynamic model is nonsingular so that the simple conventional Luenberger observer could be employed to precisely estimate state variables and fault signals for the consequent  $H_2/H_\infty$  observer-based FTC design of T-S fuzzy system with actuator and sensor faults as well as external disturbance and measurement noise.

Despite the fact that the design concept of MO control is suitable for modern industry, it is not easy to solve the corresponding multi-objective optimization problem (MOP) in general. Especially, in the fuzzy-based MOP, the computational complexity will be multiple growing according to the number of fuzzy IF-THEN rules. Among wide ranges of different algorithms of nature-inspired optimization method [30]–[33], the multi-objective evolution algorithms (MOEAs) are powerful nature-inspired optimization method to solve the MOP [34]–[36]. In general, the conventional MOEAs update design parameters by evolution algorithm (EA) to search the multi-objective vector for the Pareto optimal solutions via the non-dominated sorting and the crowded tournament selection schemes in the design parametric space [31]–[36]. Since fuzzy controller and observer of complex fuzzy systems consist of a large number of local controllers and observers, respectively, it is almost impossible to employ EA for updating these fuzzy controller and observer parameters to achieve a MOP of complex T-S fuzzy systems, such as the multi-objective  $H_2/H_\infty$  observer-based FTC of T-S fuzzy systems with actuator and sensor faults. This is why the conventional MOEAs have not been addressed on the MOP of nonlinear T-S fuzzy systems even they are very powerful in MOPs of other more simple designed systems. Besides, for the conventional MOEAs, the corresponding objective vector of child population randomly generated by crossover operation and mutation operation may exceed the real Pareto front if the current population is close to the real Pareto optimality. Clearly, if the generated child population is infeasible, it will be directly discarded. In this situation, it is much difficult to generate feasible child population while the current population is close to the real Pareto optimality [37], [38]. Hence, it is more appealing to override the bottleneck of the conventional MOEA to solve the more complex MOP such as multi-objective  $H_2/H_\infty$  observer-based FTC of T-S fuzzy systems.

In this study, a simple Luenberger observer-based FTC is designed for the T-S fuzzy system with actuator and sensor faults as well as external disturbance and measurement noise. In order to achieve the optimal robust attenuation of external disturbances on the FTC performance of the controller and observer, the optimal  $H_\infty$  observer-based FTC design is proposed to minimize the effect of the external disturbance and measurement noise on the FTC performance of control and observation. While the effects of external disturbance and measurement noise have been optimally attenuated by the  $H_\infty$  observer-based control strategy, the  $H_2$  observer-based control strategy is also proposed to achieve the optimal

quadratic control and observation simultaneously, i.e., to achieve the MOP of multi-objective  $H_2/H_\infty$  observer-based FTC of T-S fuzzy systems.

On the other hand, a reverse-order MOEA is proposed to simplify the design procedure of the complex MO  $H_2/H_\infty$  fuzzy observer-based FTC design problem. Instead of searching controller and observer parameters directly, we search the  $H_2/H_\infty$  objective vector  $(\alpha, \beta)$  directly by EA algorithm, non-dominated sorting, and crowded tournament selection scheme, and then find the corresponding controller and observer parameters by LMI TOOLBOX in MATLAB via the convex optimization algorithm indirectly. Based on the proposed reverse-order MOEA algorithm and LMI TOOLBOX in MATLAB, we could efficiently solve the complex MOP of multi-objective  $H_2/H_\infty$  observer-based FTC of T-S fuzzy system. In the future, the proposed reverse-order MOEA algorithm could be applied to other complex MOPs of nonlinear control and estimation design problem. An observer-based 3-D missile guidance system with actuator and sensor fault, due to suddenly cheating side-step maneuvering and hostile jamming, respectively, is given to illustrate the design procedure and then validate the performance of the proposed multi-objective  $H_2/H_\infty$  optimal fault-tolerant guidance control design. Besides, a multi-objective  $H_2/H_\infty$  FTC design for inverted pendulum system is carried out in comparison with state-of-the-art FTC method.

The contributions of this study are described as follows:

(I) In this study, a novel non-singular smoothed dynamic model is proposed to efficiently describe the actuator and sensor fault signals. Thus, instead of constructing the conventional singular descriptor estimator for fault signal, the simple Luenberger observer could be employed to precisely estimate state variables and actuator and sensor fault signals for the  $H_2/H_\infty$  observer-based FTC design. Further, comparing to the descriptor-based FTC design which has to solve a set of algebraic constraints, the proposed FTC design can be transformed to an equivalent LMIs-based constrained optimization problem and it is easier to be solved for practical application.

(II) Instead of using conventional MOEA to search the design parameters of fuzzy controller gain and observer gain for the multi-objective  $H_2/H_\infty$  observer-based FTC design problem, a reverse-order MOEA algorithm is proposed to directly search the optimal multi-objective vector and then the corresponding design variables of controller and observer can be easily obtained by using MATLAB LMI TOOLBOX. In the future, the proposed reverse-order MOEA algorithm could be applied to efficiently solve other complex MOP of control and estimation in the nonlinear systems or T-S fuzzy systems.

(III) To improve the rate of convergence of MOEA, a mechanism is included to deal with the problem "infeasible population generated by the mutation operator and crossover operator in MOEA. By embedding this additional mechanism in the proposed reverse-order MOEA, the infeasible population is replaced by the mean of itself and the closest

feasible population in the previous iteration. In this situation, the information of infeasible population can be utilized to find the closest feasible population for each iteration. Hence, the convergence of the proposed MOEA can be effectively improved than the conventional MOEAs.

This study is organized as follows: The T-S fuzzy system model with actuator and sensor fault are introduced in Section II. The virtual fault dynamic models are also given in Section II, too. In Section III, we develop the multi-objective optimal  $H_2/H_\infty$  observer-based FTC design for the T-S fuzzy system with sensor and actuator fault. A reverse-order MOEA for the multi-objective observer-based FTC design is proposed in Section IV. The simulation of a fault-tolerant missile guidance control design of 3-D tactical missile system and FTC design for inverted pendulum system are proposed to verify the effectiveness of the proposed method in Section V. Conclusions are given in Section VI.

*Notation:*  $A^T$ : the transpose of matrix  $A$ ;  $A \geq 0$  ( $A > 0$ ): symmetric positive semi-definite (symmetric positive definite) matrix  $A$ ;  $\|x\|$ : the Euclidean norm for the given vector  $x(t) \in \mathbb{R}^n$ ;  $\mathcal{L}_2(\mathbb{R}^+; \mathbb{R}^n) = \{v(t) : \mathbb{R}^+ \rightarrow \mathbb{R}^n \mid (\int_0^\infty v^T(t)v(t)dt)^{\frac{1}{2}} < \infty\}$ ;  $\lambda_{\max}(P)$ : the maximum eigenvalue of real-value symmetric matrix  $P$ ,  $I_a$  denotes the identity matrix with dimension  $a \times a$ . The symbol  $0_{a \times b}$  expresses the zero matrix with dimension  $a \times b$ .  $eig(A)$  denotes the set which collect the eigenvalues of matrix  $A$ .  $\mathcal{S}$  denotes the set of one-dimensional complex number.  $col[D]$  denotes the column space of matrix  $D$ .

## II. SYSTEM DESCRIPTION

We consider the continuous-time nonlinear system with actuator and sensor faults, which could be described by T-S fuzzy model. The  $i$ th fuzzy IF-THEN rule of the nonlinear system can be represented as follows [9], [10]:

If  $z_1(t)$  is  $F_{i1}$  and ... and  $z_g(t)$  is  $F_{ig}$ ,

Then

$$\dot{x}(t) = A_i x(t) + B_{u,i} u(t) + B_{a,i} f_a(t) + B_{w,i} w(t),$$

$$y(t) = C_i x(t) + D_i f_s(t) + n(t), \text{ for } i = 1, \dots, I. \quad (1)$$

where  $x(t) \in \mathbb{R}^n$  is the state vector,  $u(t) \in \mathbb{R}^{n_u}$  is the input vector,  $y(t) \in \mathbb{R}^m$  denotes the measurement output by sensors,  $f_a(t) \in \mathbb{R}^{n_a}$  and  $f_s(t) \in \mathbb{R}^{n_s}$  are the fault signal on actuators and sensors, respectively,  $w(t) \in \mathbb{R}^{n_w}$  denotes the the external disturbance and  $n(t) \in \mathbb{R}^m$  denotes the measurement noise at sensor.  $z_1(t), \dots, z_g(t)$  are the premise variables,  $F_{ij}$  is the  $i$ th fuzzy set of the  $j$ th premise variable, for  $i = 1, \dots, I$  and  $j = 1, \dots, g$ , where  $I$  is the number of fuzzy rules. The matrices  $A_i \in \mathbb{R}^{n \times n}$ ,  $B_{u,i} \in \mathbb{R}^{n \times n_u}$ ,  $B_{a,i} \in \mathbb{R}^{n \times n_a}$ ,  $B_{w,i} \in \mathbb{R}^{n \times n_w}$ ,  $C_i \in \mathbb{R}^{m \times n}$ ,  $D_i \in \mathbb{R}^{m \times n_s}$ , for  $i = 1, \dots, I$ . Thus, the overall T-S fuzzy system in (1) is inferred as follows [10]:

$$\dot{x}(t) = \sum_{i=1}^I h_i(z(t)) (A_i x(t) + B_{u,i} u(t) + B_{a,i} f_a(t) + B_{w,i} w(t)),$$

$$y(t) = \sum_{i=1}^I h_i(z(t)) (C_i x(t) + D_i f_s(t) + n(t)), \quad (2)$$

where  $z(t) = [z_1(t), \dots, z_g(t)]$ ,  $q_i(z(t)) = \prod_{j=1}^g F_{ij}(z_j(t))$  and  $h_i(z(t)) = \frac{q_i(z(t))}{\sum_{j=1}^I q_j(z(t))}$ , which satisfies  $1 \geq h_i(z(t)) \geq 0$  and  $\sum_{i=1}^I h_i(z(t)) = 1$ .

*Assumption 1:* The T-S fuzzy system in (2) is controllable and observable, i.e., the pair  $(A_i, B_{u,i})$  is controllable and the pair  $(A_i, C_i)$  is observable, for  $i = 1, \dots, I$ .

In this study, in order to efficiently estimate fault signals  $f_a(t)$  and  $f_s(t)$  by the conventional Luenberger observer for the FTC design in the sequel, a novel dynamic smoothed model is proposed for fault signals  $f_a(t)$  and  $f_s(t)$ . To begin with, based on the derivative definition of  $\dot{f}_a(t) = \lim_{h \rightarrow 0} \frac{f_a(t+h) - f_a(t)}{h}$ , the smoothed model of  $f_a(t)$  is given as follows:

$$\begin{aligned} \dot{f}_a(t) &= \frac{1}{h} (f_a(t+h) - f_a(t)) + \epsilon_{1,a}(t), \\ \dot{f}_a(t-h) &= \frac{1}{h} (f_a(t) - f_a(t-h)) + \epsilon_{2,a}(t), \\ &\vdots \\ \dot{f}_a(t-kh) &= \frac{1}{h} (f_a(t - (k-1)h) - f_a(t - kh)) \\ &\quad + \epsilon_{k,a}(t), \end{aligned} \tag{3}$$

where  $\epsilon_{1,a}(t), \dots, \epsilon_{k,a}(t)$  denote the corresponding approximation errors of derivative at different smoothed time points for actuator fault  $f_a(t)$ . The constant  $h$  is a small enough time interval. Further, in order to reduce the effect of future fault signal  $f_a(t+h)$  on the dynamic smoothed model of fault signal  $f_a(t)$ ,  $f_a(t+h)$  could be also represented by extrapolation (e.g., Lagrange extrapolation [39]) as follows:

$$f_a(t+h) = \sum_{i=0}^k a_i f_a(t-ih) + \delta_a(t), \tag{4}$$

where  $a_i, i = 0, \dots, k$  are the extrapolation coefficients,  $\delta_a(t)$  indicates the extrapolation error of  $f_a(t+h)$ . Then, we could obtain the following dynamic smoothed model of actuator fault signal  $f_a(t)$ :

$$\dot{F}_a(t) = A_{f_a} F_a(t) + \epsilon_a(t), \tag{5}$$

where  $F_a(t) = [f_a(t)^T, f_a(t-h)^T, \dots, f_a(t-kh)^T]^T$ , the smoothed model error of actuator  $\epsilon_a(t) = [(\epsilon_{1,a}(t) + \delta_a(t)/h)^T, \epsilon_{2,a}^T(t), \dots, \epsilon_{k,a}^T(t)]^T$ , and

$$A_{f_a} = \begin{bmatrix} \frac{\bar{a}_0}{h} I_{n_a} & \frac{a_1}{h} I_{n_a} & \frac{a_2}{h} I_{n_a} & \dots & \frac{a_k}{h} I_{n_a} \\ \frac{1}{h} I_{n_a} & -\frac{1}{h} I_{n_a} & 0 & \dots & 0 \\ 0 & \frac{1}{h} I_{n_a} & -\frac{1}{h} I_{n_a} & \dots & 0 \\ \vdots & & \ddots & \ddots & \vdots \\ 0 & \dots & 0 & \frac{1}{h} I_{n_a} & -\frac{1}{h} I_{n_a} \end{bmatrix},$$

where  $\bar{a}_0 = -1 + a_0$ . Similarly, the dynamic smoothed model for the sensor fault signal  $f_s(t)$  is similar to the virtual signal

model in (5) as follows:

$$\dot{F}_s(t) = A_{f_s} F_s(t) + \epsilon_s(t), \tag{6}$$

where  $F_s(t) = [f_s(t)^T, f_s(t-h)^T, \dots, f_s(t-kh)^T]^T$ , the smoothed model error of sensor  $\epsilon_s(t) = [(\epsilon_{1,s}(t) + \delta_s(t)/h)^T, \epsilon_{2,s}^T(t), \dots, \epsilon_{k,s}^T(t)]^T$  and

$$A_{f_s} = \begin{bmatrix} \frac{\bar{b}_0}{h} I_{n_s} & \frac{b_1}{h} I_{n_s} & \frac{b_2}{h} I_{n_s} & \dots & \frac{b_k}{h} I_{n_s} \\ \frac{1}{h} I_{n_s} & -\frac{1}{h} I_{n_s} & 0 & \dots & 0 \\ 0 & \frac{1}{h} I_{n_s} & -\frac{1}{h} I_{n_s} & \dots & 0 \\ \vdots & & \ddots & \ddots & \vdots \\ 0 & \dots & 0 & \frac{1}{h} I_{n_s} & -\frac{1}{h} I_{n_s} \end{bmatrix},$$

where  $\bar{b}_0 = -1 + b_0, b_i, i = 0, \dots, k$  are the extrapolation coefficients

*Remark 1:* For the T-S fuzzy system (2) with the signal faults on actuators and sensors, it is difficult to construct a suitable fault estimation scheme due to the unknown prior knowledge of the actuator faults and the sensor faults. In the traditional augmented descriptor observer design, the unknown input (i.e., the fault signal) decoupling condition cannot always be satisfied [3]. Therefore, more efforts are needed to efficiently estimate the state and fault information. In this study, unlike the conventional descriptor model [40], the nonsingular fault dynamic models of  $f_a(t)$  and  $f_s(t)$  in (5) and (6) are to be embedded in the augmented system with T-S fuzzy system in (2). In this situation, the conventional Luenberger observer could be employed to precisely estimate the state variables and actuator and sensor fault signals to efficiently compensate the effect of fault signals and external disturbance for the FTC design.

For the convenience of estimating  $x(t)$  and  $f_a(t), f_s(t)$  simultaneously, the dynamic smoothed model of fault signals in (5) and (6) could be embedded as an internal model of T-S fuzzy system in (2) as the following augmented system:

$$\begin{aligned} \dot{\bar{x}}(t) &= \sum_{i=1}^I h_i(z(t)) (\bar{A}_i \bar{x}(t) + \bar{B}_{u,i} u(t) + \bar{B}_{w,i} \bar{w}(t)), \\ y(t) &= \sum_{i=1}^I h_i(z(t)) (\bar{C}_i \bar{x}(t) + \bar{D}_i \bar{w}(t)), \end{aligned} \tag{7}$$

with the augmented state  $\bar{x}(t) = [F_a^T(t), F_s^T(t), x^T(t)]^T$ , the mapping matrix  $C_{f_a} = [I_{n_a}, 0_{n_a \times n_a}, \dots, 0_{n_a \times n_a}]$ , the vector  $\bar{w}(t) = [\epsilon_a^T(t), \epsilon_s^T(t), w^T(t), n^T(t)]^T$ , the mapping matrix  $C_{f_s} = [I_{n_s}, 0_{n_s \times n_s}, \dots, 0_{n_s \times n_s}]$  and

$$\begin{aligned} \bar{A}_i &= \begin{bmatrix} A_{f_a} & 0 & 0 \\ 0 & A_{f_s} & 0 \\ B_{a,i} C_{f_a} & 0 & A_i \end{bmatrix}, & \bar{B}_{u,i} &= \begin{bmatrix} 0 \\ 0 \\ B_{u,i} \end{bmatrix}, \\ \bar{B}_{w,i} &= \begin{bmatrix} I & 0 & 0 & 0 \\ 0 & I & 0 & 0 \\ 0 & 0 & B_{w,i} & 0 \end{bmatrix}, & \bar{C}_i &= [0 \quad D_i C_{f_s} \quad C_i], \end{aligned}$$



and  $\bar{D}_i = [0 \ 0 \ 0 \ I]$ . Before the estimating the state and actuator and sensor signals for fault tolerant control of fuzzy system in (1), we need to guarantee the augmented state  $\bar{x}(t)$  in (7) could be observable from  $y(t)$ .

*Theorem 1:* For the T-S fuzzy system in (1), if the local matrices  $(A_i, C_i)$  for  $i = 1, \dots, I$  are observable, i.e.,

$$\text{rank} \begin{bmatrix} sI_n - A_i \\ C_i \end{bmatrix} = n, \quad \text{for } s \in \mathcal{S}, \quad (8)$$

and the following conditions hold

$$\text{eig}(A_i) \cap \text{eig}(A_{f_a}) = \emptyset, \text{eig}(A_i) \cap \text{eig}(A_{f_s}) = \emptyset$$

$$\text{eig}(A_{f_s}) \cap \text{eig}(A_{f_a}) = \emptyset \quad (9)$$

$$\text{col} \begin{bmatrix} -B_{a,i}C_{f_a} \\ 0 \end{bmatrix} \cap \text{col} \begin{bmatrix} sI_n - A_i \\ C_i \end{bmatrix} = \emptyset$$

for  $s \in A_{f_a}$  (10)

$$\text{rank} \begin{bmatrix} sI_{n_a(k+1)} - A_{f_a} \\ -B_{a,i}C_{f_a} \end{bmatrix} = n_a(k+1),$$

for  $s \in \mathcal{S}$ , (11)

$$\text{rank} \begin{bmatrix} sI_{n_s(k+1)} - A_{f_s} \\ D_iC_{f_s} \end{bmatrix} = n_s(k+1),$$

for  $s \in \mathcal{S}$  (12)

then the  $i$ th augmented fuzzy system  $(\bar{A}_i, \bar{C}_i)$  in (7) is observable, for  $i = 1, \dots, I$ .

*Proof:* See Appendix A. □

*Remark 2:* The physical meaning of the conditions in (11) and (12) is that the fault state  $f_a(t)$  of dynamic smoothed model in (5) and fault state  $f_s(t)$  of dynamic smoothed model in (6) are all observable.

Suppose the following conventional fuzzy Luenberger observer is proposed to deal with the estimation of the state variables and actuator and sensor fault signals of nonlinear system in (2) or the state of the augmented system in (7):

Observer Rule  $i$ :

If  $z_1(t)$  is  $F_{i1}$  and  $\dots$  and  $z_g(t)$  is  $F_{ig}$ ,

Then

$$\begin{aligned} \dot{\hat{x}}(t) &= \bar{A}_i \hat{x}(t) + \bar{B}_{u,i} u(t) + L_i(y(t) - \hat{y}(t)), \\ \hat{y}(t) &= \bar{C}_i \hat{x}(t), \end{aligned} \quad (13)$$

where  $L_i \in \mathbb{R}^{((n_a+n_s)(k+1)+n) \times m}$  is the observer parameters for  $i = 1, \dots, I$ . The vectors  $\hat{x}(t) \in \mathbb{R}^{(n_a+n_s)(k+1)+n}$  and  $\hat{y}(t) \in \mathbb{R}^m$  are the estimated state and the estimated measurement output for the T-S fuzzy system in (7), respectively. Then the overall fuzzy observer can be designed as follows:

$$\begin{aligned} \dot{\hat{x}}(t) &= \sum_{i=1}^I h_i(z(t))(\bar{A}_i \hat{x}(t) + \bar{B}_{u,i} u(t) \\ &\quad + L_i(y(t) - \hat{y}(t))) \\ &= \sum_{i=1}^I \sum_{j=1}^I h_i(z(t))h_j(z(t))(\bar{A}_i \hat{x}(t) + \bar{B}_{u,i} u(t) \\ &\quad + L_i(\bar{C}_j(\hat{x}(t) - \hat{x}(t)) + \bar{D}_j \bar{w}(t))). \\ \hat{y}(t) &= \sum_{i=1}^I h_i(z(t))\bar{C}_i \hat{x}(t), \end{aligned} \quad (14)$$

*Remark 3:* In general, the state variables  $\bar{x}(t)$  in (7) are not accessible. Thus, the estimated state can be specified as the premise variables in the T-S fuzzy model (14), i.e.,  $z(t) = \hat{x}(t)$ .

In this article, we employ the T-S fuzzy observer-based controller to deal with the fault-tolerant controller design of the above T-S fuzzy system in (14). Thus, the  $j$ th fuzzy control rule is given as follows:

Control Rule  $j$ :

If  $z_1(t)$  is  $F_{j1}$  and  $\dots$  and  $z_g(t)$  is  $F_{jg}$ ,

$$\text{Then } u(t) = K_j \hat{x}(t), \quad (15)$$

for  $j = 1, \dots, I$ . Hence, the overall fuzzy controller can be represented as:

$$u(t) = \sum_{j=1}^I h_j(z(t))K_j \hat{x}(t), \quad (16)$$

where  $K_j \in \mathbb{R}^{n_u \times ((n_a+n_s)(k+1)+n)}$  denotes the  $j$ th fuzzy controller gain to be designed, for  $j = 1, \dots, I$ . Let us denote the estimation error as  $e(t) = \bar{x}(t) - \hat{x}(t)$ , then we can formulate the augmented fuzzy observer-based fault-tolerant control systems as follows:

$$\begin{aligned} \begin{bmatrix} \dot{\bar{x}}(t) \\ \dot{e}(t) \end{bmatrix} &= \sum_{i=1}^I \sum_{j=1}^I h_i(z(t))h_j(z(t)) \\ &\quad \times \left( \begin{bmatrix} \bar{A}_i + \bar{B}_{u,i}K_j & -\bar{B}_{u,i}K_j \\ 0 & \bar{A}_i - L_i\bar{C}_j \end{bmatrix} \begin{bmatrix} \bar{x}(t) \\ e(t) \end{bmatrix} \right. \\ &\quad \left. + \begin{bmatrix} \bar{B}_{w,i} \\ \bar{B}_{w,i} - L_i\bar{D}_j \end{bmatrix} \bar{w}(t) \right). \end{aligned} \quad (17)$$

Let us denote  $\tilde{x}(t) = [\bar{x}^T(t) \ e^T(t)]^T$  and

$$\begin{aligned} \tilde{A}_{ij} &= \begin{bmatrix} \bar{A}_i + \bar{B}_{u,i}K_j & -\bar{B}_{u,i}K_j \\ 0 & \bar{A}_i - L_i\bar{C}_j \end{bmatrix}, \\ \tilde{D}_{ij} &= \begin{bmatrix} \bar{B}_{w,i} \\ \bar{B}_{w,i} - L_i\bar{D}_j \end{bmatrix}, \end{aligned}$$

then the augmented system in (17) could be expressed as follows:

$$\dot{\tilde{x}}(t) = \sum_{i=1}^I \sum_{j=1}^I h_i(z(t))h_j(z(t))(\tilde{A}_{ij}\tilde{x}(t) + \tilde{D}_{ij}\bar{w}(t)) \quad (18)$$

which is the observer-based output feedback T-S fuzzy system. Since the augmented disturbance  $\bar{w}(t)$  due to external disturbance, modeling errors of fault signals and measurement noises in (18) will significantly influence state estimation and control performance, the following MO observer-based control is designed to  $H_\infty$  optimally attenuate the effect of  $\bar{w}(t)$  on the observer-based fault-tolerant control and  $H_2$  optimally achieve the observer-based fault-tolerant quadratic control performance simultaneously.

### III. MULTI-OBJECTIVE OPTIMAL $H_2/H_\infty$ OBSERVER-BASED FAULT-TOLERANT CONTROL FOR T-S FUZZY SYSTEM WITH ACTUATOR AND SENSOR FAULTS

In the closed-loop observer-based output feedback T-S fuzzy control system in (18), the effects of smoothed model error

of sensor and actuator faults, the external disturbance and the measurement noise in  $\bar{w}(t)$  will deteriorate the control and estimation performance of the observer-based FTC system and even lead to the instability of the fuzzy observer-based FTC system. In this situation, how to eliminate the effect of the smoothed model error of sensor and actuator faults, the external disturbance and the measurement noise in  $\bar{w}(t)$  to guarantee the robust control performance will be an important design purpose of the fuzzy observer-based fault-tolerant control system. Since  $H_\infty$  control is the most important robust control design to efficiently eliminate the effect of uncertain  $\bar{w}(t)$  on the FTC system, it will be employed to deal with the robust observer-based FTC problem for the T-S fuzzy system in (18). Let us consider the following  $H_\infty$  observer-based fault-tolerant control performance of (18):

$$H_\infty(\{L_i, K_j\}_{i,j=1}^I) = \sup_{\bar{w}(t) \in \mathcal{L}_2(\mathbb{R}^+; \mathbb{R}^{n_{\bar{w}}})} \frac{\int_0^{t_f} \tilde{x}^T(t) \tilde{Q}_1 \tilde{x}(t) dt - \tilde{x}^T(0) P \tilde{x}(0)}{\int_0^{t_f} \bar{w}^T(t) \bar{w}(t) dt}, \quad (19)$$

where  $t_f$  is the terminal time of control, the matrix  $\tilde{Q}_1 = \text{diag}\{0_{n_a(k+1) \times n_a(k+1)}, 0_{n_s(k+1) \times n_s(k+1)}, \tilde{Q}_{1,x}, \tilde{Q}_{1,e}\}$  is specified beforehand according to the design purpose with the weighting matrix  $\tilde{Q}_{1,x} \geq 0$  on the system state  $x(t)$  and the weighting matrix  $\tilde{Q}_{1,e} \geq 0$  on the estimation error  $e(t)$ .  $n_{\bar{w}} = (n_a + n_s)(k + 1) + n_w + m$  is the dimension of  $\bar{w}(t)$ . The term  $\tilde{x}^T(0) P \tilde{x}(0)$  for some  $P = P^T > 0$  in the numerator of (19) is used to deduct the effect of initial condition  $\tilde{x}(0)$  on the  $H_\infty$  control and estimation performance. The main purpose of  $H_\infty$  control and estimation performance is to eliminate the effect of external disturbance and measurement noise on the control and estimation performance of the observer-based T-S fuzzy FTC system in (18).

Most of the time, the nonlinear system is always in the normal condition without the occurrence of external disturbance and measurement noise. The consideration of  $H_\infty$  FTC design is not enough and it may lead to a very conservative design. Hence, the following  $H_2$  optimal control and estimation design, without the consideration of disturbance signal  $\bar{w}(t)$ , is more appealing for control engineers to achieve an optimal quadratic observer-based fault-tolerant control via a proper choice of weighting matrices:

$$H_2(\{L_i, K_j\}_{i,j=1}^I) = \int_0^{t_f} \tilde{x}^T(t) \tilde{Q}_2 \tilde{x}(t) + u^T(t) \tilde{R}_2 u(t) dt, \quad (20)$$

where  $\tilde{R}_2$  is the weighting matrix of control effort,  $\tilde{Q}_2 = \text{diag}\{0_{n_a(k+1) \times n_a(k+1)}, 0_{n_s(k+1) \times n_s(k+1)}, \tilde{Q}_{2,x}, \tilde{Q}_{2,e}\}$  with the weighting matrix  $\tilde{Q}_{2,x} \geq 0$  on the system state  $x(t)$  and the weighting matrix  $\tilde{Q}_{2,e} \geq 0$  on the estimation error  $e(t)$ . The weighting matrices  $\tilde{Q}_2 \geq 0$  and  $\tilde{R}_2 > 0$  are specified beforehand according to the design purpose of FTC. Thus, the multi-objective optimal  $H_2/H_\infty$  observer-based FTC design problem for the fuzzy observer-based control

system in (18) is given as follows:

$$\begin{aligned} \min_{L_i, K_j} & (H_2(\{L_i, K_j\}_{i,j=1}^I), H_\infty(\{L_i, K_j\}_{i,j=1}^I)) \\ & j, i=1, \dots, I \\ \text{Subject to} & (18). \end{aligned} \quad (21)$$

In the above MOP, there exist a set of Pareto optimal solutions for multi-objective optimal  $H_2/H_\infty$  observer-based FTC design problem in the Pareto optimal sense. In general, it is not easy to solve the MOP in (21) directly. Thus, in this study, an indirect method is proposed in the following to solve the MOP in (21) for multi-objective optimal  $H_2/H_\infty$  FTC design from the suboptimal perspective:

$$\begin{aligned} \min & (\alpha, \beta) \\ & \{L_i, K_j\}_{i,j=1}^I \\ & \alpha > 0, \beta > 0 \\ \text{Subject to} & H_2(\{L_i, K_j\}_{i,j=1}^I) \leq \alpha, \\ & H_\infty(\{L_i, K_j\}_{i,j=1}^I) \leq \beta. \end{aligned} \quad (22)$$

Since the MOP needs to minimize the multiple objective functions simultaneously, we use the Pareto domination instead of the conventional minimization. The solution of MOP in (22) is a set of fuzzy control and observer parameters  $\{L_i^*, K_j^*\}_{i,j=1}^I$  with the corresponding non-dominated objective vector  $(\alpha^*, \beta^*)$ . Before the further analysis, the following fundamental definitions are provided:

**Definition 1 (Pareto Dominance [35]):** For the MOP in (22), a solution  $\{L_i^1, K_j^1\}_{i,j=1}^I$  with feasible objective vector  $(\alpha^1, \beta^1)$  is said to dominate another solution  $\{L_i^2, K_j^2\}_{i,j=1}^I$  with feasible objective vector  $(\alpha^2, \beta^2)$  if and only if  $\alpha^1 \leq \alpha^2$  and  $\beta^1 \leq \beta^2$  and at least one of two inequalities with strict inequality.

**Definition 2 (Pareto Optimal Solution [35]):** For the MOP in (22), the solution  $\{L_i^*, K_j^*\}_{i,j=1}^I$  with the corresponding objective vector  $(\alpha^*, \beta^*)$  is a Pareto optimal solution if and only if it could not be dominated by any other solution.

**Remark 4:** Under the concept of Pareto optimal solution [35], the Pareto optimal solution of the MOP in (21) is not unique, i.e., there exist a set of Pareto optimal solutions for the MOP in (21). Since there exist multiple solutions, it is not easy to solve the MOP in (21) by conventional optimization techniques.

**Theorem 2:** The MOP in (22) is equivalent to the MOP in (21) if the Pareto optimal solutions are achieved.

**Proof:** The proof is simple if we could prove that two inequalities in the constraints of (22) become equalities when the optimization objective vector  $(\alpha^*, \beta^*)$  is achieved. We will prove this by contradiction. Suppose the inequality constraints in (22) are strictly held for a Pareto optimal solution  $(\alpha', \beta')$ , i.e., there exists a Pareto optimal solution  $(\alpha', \beta')$  such that  $H_2(\{L_i', K_j'\}_{i,j=1}^I) < \alpha'$  and  $H_\infty(\{L_i', K_j'\}_{i,j=1}^I) < \beta'$  are strictly held. However, we can find  $(\alpha^*, \beta^*)$  such that  $H_2(\{L_i', K_j'\}_{i,j=1}^I) = \alpha^*$  and  $H_\infty(\{L_i', K_j'\}_{i,j=1}^I) = \beta^*$ . This immediately shows that the solution  $(\alpha', \beta')$  is dominated by  $(\alpha^*, \beta^*)$  and  $(\alpha', \beta')$  is not the Pareto optimal solution in (22), which completes the inference of contradiction.  $\square$

Based on Theorem 2, the MOP for multi-objective  $H_2/H_\infty$  observer-based FTC problem becomes the MOP in (22). Before we solve the MOP in (22), the following lemma is given:

*Lemma 1 [41]: For any two vectors  $x \in \mathbb{R}^n, y \in \mathbb{R}^m$  and positive matrix  $P$ , we have*

$$x^T P y + y^T P x \leq \frac{1}{\rho^2} x^T P P x + \rho^2 y^T y,$$

where  $\rho$  is any nonzero real number.

*Theorem 3: The MOP in (22) for the multi-objective optimal  $H_2/H_\infty$  fault-tolerant control design can be transformed to the following MOP:*

$$\min_{\substack{\alpha > 0, \beta > 0 \\ \{L_i, K_j\}_{i,j=1}^I}} (\alpha, \beta) \quad (23)$$

$$\text{subject to } \tilde{A}_{ij}^T P + P \tilde{A}_{ij} + \tilde{Q}_2 + \tilde{K}_j^T \tilde{R}_2 \tilde{K}_j \leq 0, \quad (24)$$

$$\tilde{x}^T(0) P \tilde{x}(0) \leq \alpha, \quad (25)$$

$$P \tilde{A}_{ij} + \tilde{A}_{ij}^T P + \tilde{Q}_1 + \frac{1}{\beta} P \tilde{D}_{ij} \tilde{D}_{ij}^T P \leq 0,$$

$$\text{where } \tilde{K}_j = [K_j, -K_j]$$

$$\forall i, j = 1, \dots, I. \quad (26)$$

*Proof:* Please refer to Appendix B.  $\square$

By choosing the general Lyapunov function  $V(\tilde{x}(t)) = \tilde{x}^T(t) P \tilde{x}(t)$  with positive definite matrix  $P > 0$ , the multi-objective optimal  $H_2/H_\infty$  FTC design can be transformed to the MOP in (23)–(26). However, since the constraints in (24)–(26) are bilinear constraints, it can not be solved directly by any current optimization technique. Thus, by choosing the Lyapunov function for the augmented fuzzy observer-based control system in (18) as the sums of Lyapunov functions of two sub-systems, i.e.,  $V(\tilde{x}(t)) = \tilde{x}^T(t) P_1 \tilde{x}(t) + e^T(t) P_2 e(t)$  with  $P_1 > 0$  and  $P_2 > 0$ , the design problem can be transformed to the MOP in (28)–(31) and it can be easily solved by MATLAB LMI TOOLBOX with the proposed two-step design procedure and reverse-order MOEA in the sequel. To begin with, some decoupling techniques are employed for the weighting matrices  $\tilde{Q}_1$  of  $H_\infty$  control performance and  $\tilde{Q}_2$  of  $H_2$  control performance as follows:

$$\tilde{Q}_1 = \begin{bmatrix} \tilde{Q}_{1,\tilde{x}} & 0 \\ 0 & \tilde{Q}_{1,e} \end{bmatrix}, \quad \tilde{Q}_2 = \begin{bmatrix} \tilde{Q}_{2,\tilde{x}} & 0 \\ 0 & \tilde{Q}_{2,e} \end{bmatrix}, \quad (27)$$

where the matrices  $\tilde{Q}_{1,\tilde{x}} = \text{diag}\{0_{n_a(k+1) \times n_a(k+1)}, 0_{n_s(k+1) \times n_s(k+1)}, \tilde{Q}_{1,x}\}$ ,  $\tilde{Q}_{2,\tilde{x}} = \text{diag}\{0_{n_a(k+1) \times n_a(k+1)}, 0_{n_s(k+1) \times n_s(k+1)}, \tilde{Q}_{2,x}\}$ . Thus, we can get the following result:

*Theorem 4: The MOP in (23) can be transformed to the following BMIs-constrained MOP:*

$$(\alpha^*, \beta^*) = \min_{\substack{\alpha > 0, \beta > 0 \\ \{K_j, L_i\}_{i,j=1}^I}} (\alpha, \beta) \quad (28)$$

subject to

$$\begin{bmatrix} \Delta''_{2,1} & -\bar{B}_{u,i} K_j & W_1 K_j^T & W_1 (\tilde{Q}_{2,\tilde{x}})^{\frac{1}{2}} \\ * & \Delta''_{2,2} & -K_j^T & 0 \\ * & * & -\bar{R}_2^{-1} & 0 \\ * & * & * & -I \end{bmatrix} \leq 0, \quad (29)$$

$$\begin{bmatrix} e^T(0) P_2 e(0) - \alpha & \tilde{x}^T(0) \\ \tilde{x}(0) & -W_1 \end{bmatrix} \leq 0, \quad (30)$$

$$\begin{bmatrix} \Delta''_{\infty,1} & -\bar{B}_{u,i} K_j & \bar{B}_{w,i} & W_1 (\tilde{Q}_{1,\tilde{x}})^{\frac{1}{2}} \\ * & \Delta''_{\infty,2} & P_2 \bar{B}_{w,i} - P_2 L_i \bar{D}_j & 0 \\ * & * & -\beta I & 0 \\ * & * & * & -I \end{bmatrix} \leq 0 \quad (31)$$

for  $i, j = 1, \dots, I$ , where  $\Delta''_{2,1} = \bar{A}_i W_1 + \bar{B}_{u,i} K_j W_1 + W_1 \bar{A}_i^T + W_1 K_j^T \bar{B}_{u,i}^T$ ,  $\Delta''_{2,2} = P_2 \bar{A}_i - P_2 L_i \bar{C}_j + \bar{A}_i^T P_2 - \bar{C}_j^T L_i^T P_2 + \tilde{Q}_{2,e}$ ,  $\Delta''_{\infty,1} = \bar{A}_i W_1 + \bar{B}_{u,i} K_j W_1 + W_1 \bar{A}_i^T + W_1 K_j^T \bar{B}_{u,i}^T$ ,  $\Delta''_{\infty,2} = P_2 \bar{A}_i - P_2 L_i \bar{C}_j + \bar{A}_i^T P_2 - \bar{C}_j^T L_i^T P_2 + \tilde{Q}_{1,e}$ .

*Proof:* see Appendix C.  $\square$

If we could solve  $(\alpha^*, \beta^*)$  of the MOP in (28)–(31) with the corresponding Pareto optimal solution  $\{W_1^*, P_2^*, \{L_i^*, K_j^*\}_{i,j=1}^I\}$ , then we could obtain the fuzzy controller parameters  $K_j^*$  in (16) and fuzzy observer parameters  $L_i^*$  in (14) for the following fuzzy observer-based FTC scheme:

$$\begin{aligned} \dot{\hat{x}}(t) &= \sum_{i=1}^I h_i(z(t)) \bar{A}_i \hat{x}(t) + \bar{B}_{u,i} u(t) + L_i^*(y(t) - \hat{y}(t)), \\ u(t) &= \sum_{j=1}^I h_j(z(t)) K_j^* \hat{x}(t), \quad \text{for } i, j = 1, \dots, I \end{aligned} \quad (32)$$

*Remark 5: (i) If we only consider the optimal  $H_2$  observer-based FTC of T-S fuzzy system, then the MOP in (28) is reduced to the following single-objective optimization problem (SOP):*

$$\alpha^+ = \min_{\substack{W_1 > 0, P_2 > 0 \\ \{K_j, L_i\}_{i,j=1}^I, \alpha > 0}} \alpha \quad \text{subject to the matrix constraints in (29), (30).} \quad (33)$$

*(ii) If we only consider the optimal  $H_\infty$  observer-based FTC of T-S fuzzy system, then the MOP in (28) is reduced to the following SOP:*

$$\beta^+ = \min_{\substack{W_1 > 0, P_2 > 0 \\ \{K_j, L_i\}_{i,j=1}^I, \beta > 0}} \beta \quad \text{subject to the matrix constraints in (31).} \quad (34)$$

*Remark 6: Since the constraints in (29) and (31) are BMIs, it can not be efficiently solved via current optimization techniques. As a result, a two step-design procedure is developed to solve the MOP in (28)–(31):*

*(1) If the inequality constraints in (29) and (31) hold, then the sufficient and necessary conditions are that the diagonal*

terms of (29) and (31) must be negative. Thus, by letting  $Z_j = K_j W_1$ , we first solve the linear constraints  $\Delta_{2,1}'' < 0$  in (29) and  $\Delta_{\infty,1}'' < 0$  in (31) to obtain the the solution  $W_1^*$  and  $\{Z_i^*\}_{i=1}^l$  by using Matlab convex optimization toolbox. Once the solutions  $W_1^*$  and  $\{Z_i^*\}_{i=1}^l$  are obtained, the corresponding fuzzy controller can be constructed as  $K_j^* = Z_j^* (W_1^*)^{-1}$ .

(II) By letting  $Y_i = P_2 L_i$  with the fixed matrices  $W_2^*$  and  $\{K_j^*\}_{j=1}^l$  obtained from step 1 in (29) and (31), the constraints in (29) and (31) become linear matrix inequalities (LMIs), which is solvable by utilizing Matlab convex optimization toolbox. Thus, we can solve (29)-(31) efficiently to obtain the optimal solutions  $P_2^*$  and  $\{Y_i^*\}_{i=1}^l$ . Once the solutions  $P_2^*$  and  $\{Y_i^*\}_{i=1}^l$  are obtained, the corresponding fuzzy observer can be constructed as  $L_i^* = (P_2^*)^{-1} Y_i^*$ .

**Remark 7:** If the robust  $H_\infty$  performance in (19) is satisfied with positive definite weighting matrix  $\tilde{Q}_1$  and a prescribed disturbance attenuation level  $\beta > 0$  and the system is free of external disturbance, the left-hand side in (19) is bounded above by  $\tilde{x}^T(0)P\tilde{x}(0)$  for any time, i.e., the summation of the state energy  $\tilde{x}(t)$  from zero to infinite time is bounded. As a result, it reveals the state variables will converge to zero by the proposed controller, i.e., the asymptotically stability for fuzzy observer-based FTC system in (18) is guaranteed.

#### IV. REVERSE-ORDER MOEA FOR MULTI-OBJECTIVE OPTIMAL $H_2/H_\infty$ OBSERVER-BASED FAULT TOLERANT DESIGN OF T-S FUZZY SYSTEMS

In the conventional MOEA, the algorithm employs evolution algorithm (EA) to search the parameter of  $\{W_1, P_2, K_i, L_i\}_{i=1}^l$  to solve the MOP in (28)-(31) directly. However, there are too many fuzzy controller and observer parameters to be searched to achieve the optimal objective vector  $(\alpha^*, \beta^*)$ . Obviously, it is almost impossible to employ the conventional MOEA to MOP in (28)-(31) to solve the multi-objective  $H_2/H_\infty$  observer-based FTC design problem. Different than the conventional multi-objective evolution algorithm (MOEA) which directly searches the solutions  $\{\alpha, \beta, W_1, P_2, K_i, L_i\}_{i=1}^l$  of the multi-objective optimal  $H_2/H_\infty$  observer-based FTC design in (28), the proposed reverse-order MOEA only searches the feasible objective vectors  $(\alpha, \beta)$ . Then, by substituting the objective vectors  $(\alpha, \beta)$  into (29)–(31), the corresponding solutions  $\{K_i, L_j\}_{i,j=1}^l$  can be easily obtained by using MATLAB LMI TOOLBOX. As a result, the multi-objective optimal  $H_2/H_\infty$  observer-based FTC design in (28) can be effectively solved by the proposed reverse-order MOEA and MATLAB LMI TOOLBOX. Before further analysis of LMIs-constrained MOP in (28)-(31), some fundamental definitions of MOP are given in the following:

**Definition 3** [35]: For the LMIs-constrained MOP (28)-(31) for multi-objective  $H_2/H_\infty$  observer-based FTC design in the T-S fuzzy system with actuator and sensor faults in (1), the ideal objective vector is defined as  $(\alpha^+, \beta^+)$  where

$\alpha^+$  and  $\beta^+$  can be obtained by solving the SOP in (33) and (34), respectively.

**Definition 4** [35]: For the LMIs-constrained MOP in (28)-(31), the solution  $\{W_1^*, P_2^*, \{K_j^*, L_i^*\}_{i,j=1}^l\}$  with the corresponding objective vector  $(\alpha^*, \beta^*)$  is called the Pareto optimal solution if there does not exist any feasible solution  $\{W_1, P_2, \{K_j, L_i\}_{i,j=1}^l\}$  with the corresponding objective vector  $(\alpha, \beta)$  that dominates the solution  $\{W_1^*, P_2^*, \{K_j^*, L_i^*\}_{i,j=1}^l\}$ .

**Definition 5** [35]: For the LMIs-constrained MOP in (28)-(31), the Pareto optimal solution set is defined as follows:

$$\Omega_{Opt} = \left\{ \left. \begin{array}{l} \text{The feasible solution} \\ \text{in (28)-(31)} \\ \text{is not dominated} \\ \text{by other feasible} \\ \text{solutions.} \end{array} \right\| \{W_1^*, P_2^*, \{K_j^*, L_i^*\}_{i,j=1}^l\} \right\},$$

i.e., the Pareto optimal solution set collects the Pareto optimal solutions for the MOP in (28)-(31).

**Definition 6** [35]: For the LMIs-constrained MOP in (28)-(31), the Pareto front is defined as follows:

$$\Omega_{Front} = \left\{ (\alpha^*, \beta^*) \left\| \begin{array}{l} \text{The objective vector} \\ (\alpha^*, \beta^*) \text{ of the solution} \\ \{W_1^*, P_2^*, \{K_j^*, L_i^*\}_{i,j=1}^l\} \in \Omega_{Opt} \end{array} \right. \right\},$$

i.e., the Pareto front  $\Omega_{Front}$  collects the objective vectors of Pareto optimal solutions in  $\Omega_{Opt}$ .

Once the Pareto front  $\Omega_{Front}$  is obtained, the corresponding fuzzy controller gains  $\{K_j^*\}_{j=1}^l$  and fuzzy observer gain  $\{L_i^*\}_{i=1}^l$  can be constructed for the multi-objective  $H_2/H_\infty$  fault-tolerant control of T-S fuzzy system with actuator and sensor failure. Based on the above analysis, a design procedure based on the proposed reverse-order MOEA method for the multi-objective optimal  $H_2/H_\infty$  observer-based FTC design of T-S fuzzy system with actuator and sensor faults is given in detail:

#### Design procedure of the multi-objective $H_2/H_\infty$ observer-based FTC for the T-S fuzzy system

- **Step 1:** Choose the searching region  $R = [\alpha_{low}, \alpha_{up}] \times [\beta_{low}, \beta_{up}]$ . The objective vector  $[\alpha_{low}, \beta_{low}]$  at the low bound can be obtained by solving two SOPs in (33) and (34), i.e.,  $\alpha_{low} = \alpha^+, \beta_{low} = \beta^+$ . Give the population number  $N_p$ , iteration number  $N_i$ , the crossover rate  $C_r$ , the mutation rate  $C_m$  of EA in the proposed reverse-order MOEA. Set the iteration index as  $j = 1$ .
- **Step 2:** Randomly generate the feasible objective vector  $\{(\alpha_i, \beta_i)\}_{i=1}^{N_p}$  from the searching region  $R$  by examining whether  $\{(\alpha_i, \beta_i)\}_{i=1}^{N_p}$  are feasible or not in LMI constraints in (29)–(31). Define the parent set as  $P_{Parent}^j = \{(\alpha_i, \beta_i)\}_{i=1}^{N_p}$ .
- **Step 3:** Employ crossover operator and mutation operator for the parent set  $P_{Parent}^j$  and produce  $N_p$  child population, i.e.,  $\{(\tilde{\alpha}_i, \tilde{\beta}_i)\}_{i=1}^{N_p}$ . Define the child set as  $P_{child}^j = \{(\tilde{\alpha}_i, \tilde{\beta}_i)\}_{i=1}^{N_p}$ . If there exists a child population  $(\tilde{\alpha}, \tilde{\beta})$



which is not feasible for the constraints in (29)-(31), then a population  $(\alpha, \beta)$  from the parent set which is most closest to  $(\tilde{\alpha}, \tilde{\beta})$  is selected and the child population is replaced by  $\frac{1}{2}(\alpha + \tilde{\alpha}, \beta + \tilde{\beta})$ . The mechanism will be repeatedly executed until the fixed child population is feasible for the constraints in (29)-(31).

- **Step 4:** Apply the nondominating sorting operator to the set  $P_{Parent}^j \cup P_{child}^j$  to obtain the corresponding non-dominated front  $\mathcal{F}^j = \{\mathcal{F}_1^j, \mathcal{F}_2^j, \dots\}$ .
- **Step 5:** Apply the crowded comparison assignment operator to the sets  $\mathcal{F}_i^j$  and generate the corresponding crowding distance of each element in  $\mathcal{F}_i^j$ , for  $i = 1, \dots$ . Based on their crowding distance, the sets  $\{\mathcal{F}_i^j\}_{i \in \mathbb{N}}$  can be sorted in descending order.
- **Step 6:** Let  $t_j \in \mathbb{N}$  be the minimum positive integer such that  $\sum_{i=1}^{t_j} |\mathcal{F}_i^j| > N_p$  where  $|S|$  denotes the cardinality of the set  $S$ , i.e.,  $t_j = \arg \min_{t_j \in \mathbb{N}} \sum_{i=1}^{t_j} |\mathcal{F}_i^j| > N_p$ . Update the iteration index  $j = j + 1$  and let the parent set  $P_{Parent}^j = \{\mathcal{F}_i^j\}_{i=1}^{t_j-1} \cup \tilde{\mathcal{F}}_{t_j}^j$  for the next iteration where  $\tilde{\mathcal{F}}_{t_j}^j$  is the set containing the first  $G^j$  elements in  $\mathcal{F}_{t_j}^j$  and  $G^j = N_p - \sum_{i=1}^{t_j-1} |\mathcal{F}_i^j|$ .
- **Step 7:** Repeat **Step 3** to **Step 6** until the iteration index  $j = N_i$  and set the final population  $P_{Parent}^{N_i} = \Omega_{Front}$  as the Pareto front.
- **Step 8:** Choose a desired Pareto optimal objective vector  $(\alpha^*, \beta^*) \in \Omega_{Front}$  according to the one's own preference with the corresponding Pareto optimal solution  $\{W_1^*, P_2^*, \{K_j^*, L_i^*\}_{i,j=1}^I\}$  of the MOP in (28)-(31). Once the "preferable" optimal solution is selected, the multi-objective optimal fuzzy observer-based fault-tolerant controller in (32) can be constructed as  $\{K_j^*\}_{j=1}^I$  and  $\{L_i^*\}_{i=1}^I$  for the multi-objective  $H_2/H_\infty$  observer-based FTC in (32) of the T-S fuzzy systems in (2).

The detailed crossover operator, mutation operator, nondominating sorting operator and crowded comparison operator are defined as follows:

**Crossover Operator:**

- (I) Define two populations  $(\alpha_1, \beta_1), (\alpha_2, \beta_2) \in \mathbb{R}^2$  and randomly generate a number  $r \in [0, 1]$ .
- (II) The crossover operator  $f_C((\alpha_1, \beta_1), (\alpha_2, \beta_2))$  is defined as follows:

$$f_C((\alpha_1, \beta_1), (\alpha_2, \beta_2)) = \begin{cases} (\alpha_1, \beta_2) & \text{if } r < C_r \\ \frac{1}{2}(\alpha_1 + \alpha_2, \beta_1 + \beta_2), o.w. \end{cases}$$

where  $C_r \in [0, 1]$  is crossover rate.

**Mutation Operator:**

- (I) Define one population  $(\alpha, \beta) \in \mathbb{R}^2$  and randomly generate two numbers  $r_1, r_2 \in [0, 1]$ .
- (II) The mutation operator  $f_M((\alpha, \beta))$  is defined as follows:

$$f_M((\alpha, \beta)) = \begin{cases} (\alpha, \beta), & \text{if } r_1 \geq C_r, r_2 \geq C_m \\ (\alpha + d_1, \beta), & \text{if } r_1 \leq C_r, r_2 \geq C_m \\ (\alpha, \beta + d_2), & \text{if } r_1 \geq C_r, r_2 \leq C_m \\ (\alpha + d_1, \beta + d_2), & \text{if } r_1 \leq C_r, r_2 \leq C_m \end{cases}$$

where  $C_m \in [0, 1]$  denotes mutation rate,  $d_1 = 1 - (2(1 - r_1))^{\frac{1}{5}}$ ,  $d_2 = 1 - (2(1 - r_2))^{\frac{1}{5}}$ .

**Crowded comparison assignment operator:**

- (I) Give a finite set  $\mathcal{I}$  with the cardinality  $l = |\mathcal{I}|$  and set  $\{I_i = 0\}_{i=1}^l$
- (II) Set the objective index  $j = 1$ .
- (III) Sort  $\mathcal{I}$  in the descending order according to their  $j$ th objective value.
- (IV) Assign the values to the first element  $I_1$  and last element  $I_l$  in the sorted set  $\mathcal{I}$  as follows:

$$I_1 = \infty, I_l = \infty,$$

- (V) Assign the values to the elements  $\{I_i\}_{i=2}^{l-1}$  in the sorted set  $\mathcal{I}$ :

$$I_i = I_i + (f_j^{i+1} - f_j^{i-1}) / (f_j^{\max} - f_j^{\min}) \\ i = 2, \dots, l - 1$$

where  $f_j^{i+1}$  and  $f_j^{i-1}$  are the  $j$ th objective value of the  $i + 1$ th element and  $i - 1$ th element in sorted set  $\mathcal{I}$ , respectively, and  $f_j^{\max}$  and  $f_j^{\min}$  are the maximum  $j$ th objective value and minimum  $j$ th objective value in the sorted set  $\mathcal{I}$ , respectively.

- (VI) Update the objective index  $j = 2$  and repeat Steps (III)-(V).

**Nondominating sorting operator:**

- (I) Given a set  $\mathcal{P}$ . For each element  $p \in \mathcal{P}$ , generate the corresponding counter index  $n_p$  and domination set  $S_p$  as follows:

$$S_p = \{q \parallel q \in \mathcal{P}, p < q\} \\ n_p = |\{q \parallel q \in \mathcal{P}, q \leq p\}|$$

where  $|S|$  denotes the cardinality of set  $S$ .

- (II) Define the first domination front  $F_1$  as

$$F_1 = \{p \parallel p \in \mathcal{P}, n_p = 0\}$$

and the  $j$ th domination front  $F_j$  as

$$F_j = \left\{ q \parallel p \in F_{j-1}, q \in S_p, n_q = \sum_{i=1}^{j-1} |F_i| \right\}$$

, for  $j \in \mathbb{N}$ .

To sum up, the multi-objective optimal  $H_2/H_\infty$  FTC design problem is transformed to the BMIs-constrained multi-objective problem (MOP). Consequently, the BMIs-constrained MOP can be solved by utilizing the proposed reverse order MOEA and MATLAB LMI TOOLBOX.

*Remark 8: The computation complexity of the proposed reverse-order MOEA for LMIs-constrained MOP in (28)-(31) is about  $O(n^2 IN_i N_p^2)$ , which includes  $O(n^2 I)$  in solving two-step LMIs in (29)-(31),  $O(N_i N_p^2)$  in the reverse-order MOEA, where  $I$  is the number of fuzzy rules,  $n$  is the dimension of positive-definite matrix  $P$ ,  $N_p$  is the population number and  $N_i$  is the iteration number.*

*Remark 9: Since the augmented system in (18) includes the smoothed model of actuator signal and sensor signal, the dimension of augmented system will be enlarged if we use more points to extrapolate the actuator fault  $f_a(t + h)$  and*

sensor fault  $f_s(t + h)$ . As a result, the computing complexity directly depends on the dimension of smoothed model of actuator and sensor signals.

**Remark 10:** In the proposed reverse-order MOEA for multi-objective  $H_2/H_\infty$  observer-based FTC design, the designer should give the following parameters for MOEA: (i) Searching region  $R = [\alpha_{low}, \alpha_{up}] \times [\beta_{low}, \beta_{up}] \in \mathbb{R}^2$  with  $\alpha_{low} \in \mathbb{R}_{\geq 0}$ ,  $\alpha_{up} \in \mathbb{R}_{\geq 0}$ ,  $\beta_{low} \in \mathbb{R}_{\geq 0}$  and  $\beta_{up} \in \mathbb{R}_{\geq 0}$  (II) Population number  $N_p \in \mathbb{N}$  (III) Iteration number  $N_i \in \mathbb{N}$  (IV) Crossover rate  $C_r \in [0, 1]$  (V) Mutation rate  $C_m \in [0, 1]$ . On the other hand, at the start of the algorithm,  $N_p$  populations are randomly generated from the searching region  $R$  and there are set as the initial population

**Remark 11:** Recently, with the advance of interpolation methods, the nonlinear inequality constraint can be equivalently transformed to a combination of local linearized matrix inequalities with corresponding interpolation functions, e.g., Fuzzy interpolation method, Global linearization method. As a result, by utilizing these interpolation methods, the proposed reverse-order MOEA can be applied to general MOPs with nonlinear inequality constraints, e.g., multi-objective optimal controller design for nonlinear system.

**Remark 12:** In the proposed reverse-order MOEA, the initial populations are randomly generated from the predefined searching region. Clearly, if the initial populations are close to the real Pareto front, the MOEA will take less time to approach the real Pareto front, i.e., the global optimality. As a result, the convergence of proposed reverse-order MOEA is related to the choosing of searching region. In this study, the searching region is defined as  $R = [\alpha_{low}, \alpha_{up}] \times [\beta_{low}, \beta_{up}]$  where  $\alpha_{low}$  and  $\beta_{low}$  can be obtained by solving two SOPs in (33) and (34). On the other hand,  $\alpha_{up}$  and  $\beta_{up}$  can be chosen as several times of  $\alpha_{low}$  and  $\beta_{low}$ , respectively, e.g.,  $\alpha_{up} = \theta \alpha_{low}$ , for some  $\theta \in \mathbb{R}_+$ . In this situation, the randomly generated initial populations will fall into the feasible region of the constraints in (24)–(26).

## V. SIMULATION EXAMPLE

To illustrate the design procedure and to validate the performance of proposed MO  $H_2/H_\infty$  observer-based FTC scheme, two simulation examples are provided. A tactical missile guidance system suffer from actuator and sensor fault signals is given. Based on the proposed smoothed model, the fault signals are embedded in an augmented missile system. Then the proposed MO  $H_2/H_\infty$  observer-based FTC control problem is given to tactical missile guidance system. Finally, the MO optimal  $H_2/H_\infty$  observer-based FTC design problem is transformed to the BMIs-constrained multi-objective problem MOP which can be easily solved by utilizing the proposed reverse-order MOEA and MATLAB LMI TOOLBOX. On the other hand, the FTC design problem of balancing and swing-up of an inverted pendulum on a cart is considered with a comparison between the proposed method and conventional FTC design in [46].

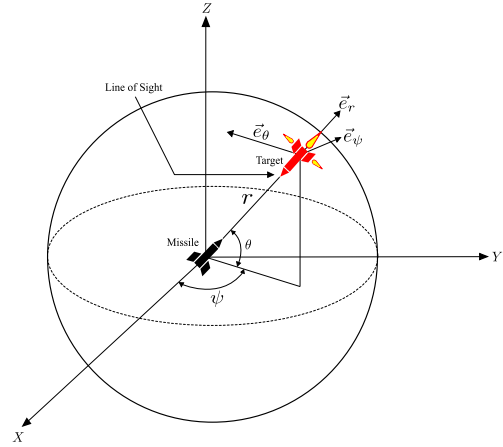


FIGURE 1. 3-D pursuit-evasion geometry in the missile guidance system.

**Example 1:** Consider the 3-D missile guidance system in the spherical coordinate  $(r, \psi, \theta)$  with the origin fixed at the missile. The pursuit-evasion geometry between the missile such as Patriot at the origin and the target such as incoming ballistic missile is shown in Fig. 1. Let  $(\vec{e}_r, \vec{e}_\psi, \vec{e}_\theta)$  be the unit vector along the coordinate axis. The 3-D relative velocity is obtained through the differentiation of the relative distance vector  $\vec{r}$  along with the line of sight (LOS) as follows [42], [44]:

$$\dot{\vec{r}} = \dot{r}\vec{e}_r + r\dot{\psi}\cos(\theta)\vec{e}_\psi + r\dot{\theta}\vec{e}_\theta \quad (35)$$

Hence, the relative acceleration at the direction of  $\vec{e}_r, \vec{e}_\psi$  and  $\vec{e}_\theta$  can be obtained by differentiating the above equation in the following:

$$\begin{aligned} \ddot{r} - r\dot{\theta}^2 - r\dot{\psi}^2\cos^2\theta &= w_r \\ r\ddot{\psi}\cos\theta + 2\dot{r}\dot{\psi}\cos\theta - 2r\dot{\theta}\dot{\psi}\sin\theta &= w_\psi - u_\psi \\ r\ddot{\theta} + 2\dot{r}\dot{\theta} + r\dot{\psi}^2\cos\theta\sin\theta &= w_\theta - u_\theta \end{aligned} \quad (36)$$

where  $u_\psi$  and  $u_\theta$  are the control inputs;  $w_r, w_\psi$  and  $w_\theta$  are the target acceleration vectors. Therefore, the kinematic between the missile and target in (36) can be represented by the following state space system:

$$\begin{aligned} \dot{x}(t) &= F(x(t)) + B_u u(t) + B_w w(t) \\ y(t) &= Cx(t) + n(t) \end{aligned} \quad (37)$$

where  $x(t) = [r(t), \psi(t), \theta(t), v_r(t), v_\psi(t), v_\theta(t)]^T$  denotes the state vector,  $F(x(t))$  denotes the vector field,  $u(t) = [u_\psi(t), u_\theta(t)]^T$  denotes the missile acceleration vector due to the guidance control and  $w(t) = [w_r(t), w_\psi(t), w_\theta(t)]^T$  denotes the target acceleration vector, which is unavailable and is considered as the external disturbance to the missile guidance system.  $y(t)$  denotes the measurement output of missile by laser sensor with measurement noise  $n(t)$ . The detailed information of these matrices are given

as follows:

$$F(x(t)) = \begin{bmatrix} \frac{v_r}{v_\psi} \\ r \cos(\theta) \\ \frac{v_\theta}{r} \\ \frac{v_\psi^2 + v_\theta^2}{r} \\ \frac{v_\psi(v_\theta \tan \theta - v_r)}{r} \\ \frac{-(v_r v_\theta + v_\psi^2 \tan \theta)}{r} \end{bmatrix}, \quad B_u = \begin{bmatrix} 0_{4 \times 2} \\ -I_2 \end{bmatrix},$$

$$B_w = \begin{bmatrix} 0_{3 \times 3} \\ I_3 \end{bmatrix}, \quad C = I_6$$

To avoid the attack of the tactical missile such as Patriot, the target will generate jamming signal to interfere with the laser sensor through the wireless channel, which will lead to an equivalent sensor fault signal. On the other hand, the target will perform sudden side-step maneuvering through its two-side jets, which will lead to an equivalent actuator fault in the missile system. By considering the sensor and actuator faults by hostile jamming and sudden side-step maneuvering, respectively, the missile guidance system in (37) with actuator and sensor fault should be revised as:

$$\begin{aligned} \dot{x}(t) &= F(x(t)) + B_u u(t) + B_w w(t) + B_a f_a(t) \\ y(t) &= Cx(t) + n(t) + Df_s(t) \end{aligned} \quad (38)$$

where  $f_a(t) \in \mathbb{R}$  denotes actuator fault due to sudden side-step maneuvering through two-side jets in the target and  $f_s(t) \in \mathbb{R}$  denotes the sensor fault of missile due to hostile jamming from target. The corresponding fault matrices are given as follows:

$$B_a = [0, 0, 0, 0, 1, 1]^T, \quad D = [0, 0, 0, 1, 1, 1]^T$$

In this simulation example, the following fuzzy premise variables are chosen  $z_1(t) = r(t)$ ,  $z_2(t) = \theta(t)$ ,  $z_3(t) = v_\psi(t)$  and  $z_4(t) = v_\theta(t)$  with the corresponding fuzzy operation points:

$$\begin{aligned} r_i &= 599.7, \text{ for } i = 1 - 24, r_i = 2560, \text{ for } i = 25 - 48 \\ \theta_i &= -0.6452 \text{ for } i = 1 - 12, 25 - 36 \\ \theta_i &= 1.2872 \text{ for } i = 13 - 24, 37 - 48 \\ v_{\psi,i} &= -50 \text{ for } i = 1 - 4, 13 - 16, 25 - 38, 37 - 40 \\ v_{\psi,i} &= 75.6 \text{ for } i = 5 - 8, 17 - 20, 29 - 32, 41 - 44 \\ v_{\psi,i} &= 551.1 \text{ for } i = 9 - 12, 20 - 24, 33 - 36, 45 - 48 \\ v_{\theta,i} &= -121 \text{ for } i = 1 + 4s, v_{\theta,i} = 0 \text{ for } i = 2 + 4s \\ v_{\theta,i} &= 135.3 \text{ for } i = 3 + 4s, v_{\theta,i} = 310.5 \text{ for } i = 4 + 4s \\ \text{where } s &= 0 - 11 \end{aligned}$$

Also, the  $i$ th IF-THEN rule of T-S fuzzy system for the nonlinear system in (38) is given as follows:

$$\begin{aligned} \text{If } r(t) \text{ is } r_i \text{ and } \theta(t) \text{ is } \theta_i \\ \text{and } v_\psi(t) \text{ is } v_{\psi,i} \text{ and } v_\theta(t) \text{ is } v_{\theta,i} \end{aligned}$$

Then

$$\begin{aligned} \dot{x}(t) &= A_i x(t) + B_{u,i} u(t) + B_{a,i} f_a(t) + B_{w,i} w(t) \\ y(t) &= C_i x(t) + D_i f_s(t) + n(t) \end{aligned} \quad (39)$$

and the detailed local linearized matrices  $\{A_i\}_{i=1}^{48}$  are given in [47].

To model the actuator fault and sensor fault, a 3rd order smoothed model in (5) is employed for actuator fault signal and a 3rd order smoothed model in (6) is employed for sensor fault signal as follows:

$$A_{f_a} = \begin{bmatrix} \frac{\bar{a}_0}{h} & \frac{a_1}{h} & \frac{a_2}{h} & \frac{a_3}{h} \\ \frac{1}{h} & -\frac{1}{h} & 0 & 0 \\ 0 & \frac{1}{h} & -\frac{1}{h} & 0 \\ 0 & 0 & \frac{1}{h} & -\frac{1}{h} \end{bmatrix},$$

$$A_{f_s} = \begin{bmatrix} \frac{\bar{b}_0}{h} & \frac{b_1}{h} & \frac{b_2}{h} & \frac{b_3}{h} \\ \frac{1}{h} & -\frac{1}{h} & 0 & 0 \\ 0 & \frac{1}{h} & -\frac{1}{h} & 0 \\ 0 & 0 & \frac{1}{h} & -\frac{1}{h} \end{bmatrix}.$$

with the specified extrapolation parameter parameters  $h = 10^{-3}$ ,  $\bar{a}_0 = -1 + a_0$ ,  $a_0 = 0.5$ ,  $a_1 = 0.3$ ,  $a_2 = 0.1$ ,  $a_3 = 0.1$ ,  $\bar{b}_0 = -1 + b_0$ ,  $b_0 = 0.6$ ,  $b_1 = 0.2$ ,  $b_2 = 0.1$  and  $b_3 = 0.1$ . Hence, the overall fuzzy observer-based FTC systems can be constructed as follows:

$$\dot{\tilde{x}}(t) = \sum_{i=1}^I \sum_{j=1}^I h_i(z(t)) h_j(z(t)) (\tilde{A}_{ij} \tilde{x}(t) + \tilde{D}_{ij} \tilde{w}(t)). \quad (40)$$

In the missile guidance control, when  $v_\psi(t) \rightarrow 0$  and  $v_\theta(t) \rightarrow 0$ , it means the missile and the target in the head-on condition [44]. Among three relative velocities, only the relative velocity  $v_r(t)$  along with line-of-sight (LOS) decreases the distance between the missile and the target, i.e.,  $v_r(t)$  could decrease the relative distance between missile. Therefore,  $v_r(t)$  could not be zero in the missile guidance process, i.e.  $v_r(t) \neq 0$ . In this situation, to ensure the head-on condition, the controlled output  $\eta(t) = [v_\psi(t), v_\theta(t)]^T$  to be controlled as small as possible for the missile guidance system in (38) can be obtained as:

$$\eta(t) = E x(t)$$

where

$$E = \begin{bmatrix} 0 & 0 & 0 & 0 & 1 & 0 \\ 0 & 0 & 0 & 0 & 0 & 1 \end{bmatrix}.$$

Therefore, to meet the head-on condition for the MO  $H_2/H_\infty$  observer-based fault-tolerant control, the weighing

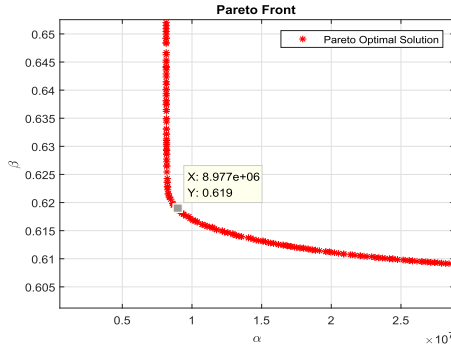


**FIGURE 2.** The Pareto front of the MO  $H_2/H_\infty$  fault-tolerant observer-based control design. In this figure, each red point represents the Pareto optimal solution in MO  $H_2/H_\infty$  fault-tolerant observer-based control design. The marked point denotes the knee solution.

matrices  $\tilde{Q}_1$  and  $\tilde{Q}_2$  in (19) and (20) should be specified as:

$$\begin{aligned} \tilde{Q}_1 &= \text{diag}\{0_{8 \times 8}, \tilde{Q}_{1,x}, \tilde{Q}_{1,e}\}, \\ \tilde{Q}_2 &= \text{diag}\{0_{8 \times 8}, \tilde{Q}_{2,x}, \tilde{Q}_{2,e}\}, \\ \tilde{Q}_{1,x} &= E^T Q_1^n E, \tilde{Q}_{2,x} = E^T Q_{2,x} E \\ Q_1^n &= \text{diag}(1, 1), Q_2^n = \text{diag}(2, 1) \\ \tilde{Q}_{1,e} &= I_{14 \times 14}, \tilde{Q}_{2,e} = I_{14 \times 14}, \tilde{R}_2 = 0.01 I_{2 \times 2} \end{aligned} \quad (41)$$

*Remark 13:* To ensure the MO  $H_2/H_\infty$  observer-based FTC performance and the head-on condition, the above weighting matrices  $\tilde{Q}_{1,x}$  and  $\tilde{Q}_{2,x}$  in  $\tilde{Q}_1$  and  $\tilde{Q}_2$  should focus on the control performance of controlled output  $\eta(t) = [v_\psi(t), v_\theta(t)]^T$ , respectively. On the other hand, to ensure the estimation performance on state variables and actuator and sensor fault signals in missile guidance system, the above weighting matrices  $\tilde{Q}_{1,e}$  and  $\tilde{Q}_{2,e}$  in  $\tilde{Q}_1$  and  $\tilde{Q}_2$  are chosen as the full rank matrix.

To apply the MOEA for the MO  $H_2/H_\infty$  observer-based FTC in (28), the design parameters of MOEA is given as:

|                         |                                      |
|-------------------------|--------------------------------------|
| Iteration Number $N_i$  | : 100                                |
| Searching Region $R$    | : $[10^6, 10^{10}] \times [0.6, 10]$ |
| Crossover Rate $C_r$    | : 0.85                               |
| Mutation Rate $C_m$     | : 0.15                               |
| Population Number $N_p$ | : 300                                |

Once the iteration number is achieved in the MOEA, the Pareto front of MO  $H_2/H_\infty$  fault-tolerant observer-based control design is plotted in the Fig. 2. In the Pareto front, each red point represents a Pareto optimal solution with the corresponding optimal  $H_2$  observer-based FTC performance and optimal  $H_\infty$  observer-based FTC performance. Since the objective vectors of obtained Pareto optimalities cannot be decreased anymore in Fig. 2, the obtained Pareto front is nearly equivalent to the real Pareto front. According to one's own demand, the designer is free to choose the one's own Pareto optimal solution. In this study, the marked point ( $8.9 \times 10^6, 0.61$ ) in Fig. 2, which is the so-called knee-solution, is chosen as the solution in this simulation.

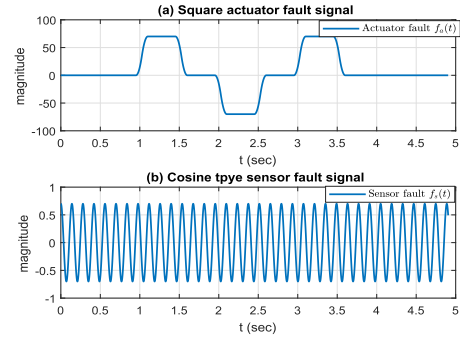


**FIGURE 3.** (a) The square actuator fault and (b) the cosine-type sensor fault signal.

In general, the knee solution has the benefit of balanced performance between the  $H_2$  performance and  $H_\infty$  performance. From the knee point, the fuzzy controllers and fuzzy observers can be constructed as  $K_j^* = Z_j^* (W_1^*)^{-1}$  and  $L_i^* = (P_2^*)^{-1} Y_i^*$ , for  $i, j = 1, \dots, 48$ . The detailed parameters of  $\{K_j^*, L_i^*\}_{i,j=1}^{48}$  can be found in [47].

In this simulation, the ramp strategy of the target is chosen as the target acceleration vectors [44]:

$$\begin{aligned} w_r(t) &= \lambda_T r(t), w_\psi(t) = \lambda_T \frac{-\dot{\theta}(t)}{\sqrt{\dot{\theta}^2(t) + \dot{\psi}(t) \cos^2 \theta(t)}} \psi(t) \\ w_\theta(t) &= \lambda_T \frac{\dot{\psi}(t) \cos \theta(t)}{\sqrt{\dot{\theta}^2(t) + \dot{\psi}(t) \cos^2 \theta(t)}} \theta(t) \end{aligned}$$

where  $\lambda_T$  denotes the target's navigation random gain within 0 to  $2G$ . The measurement noise and the initial condition of the missile guidance system in (38) are given as:

$$\begin{aligned} n(t) &= 0.5 * \cos(0.05 * t) * [1, 1, 1, 1, 1, 1]^T \\ x_0 &= [4900, \pi/3, \pi/3, -1000, 500, 500]^T \end{aligned}$$

In general, to avoid the attack of the missile, the target can perform sudden side-step maneuvering by its two-side jets and transmit the jamming signal to interfere the missile, which could lead to an equivalent actuator and sensor faults, respectively. In this simulation, the equivalent actuator fault signal due to the sudden side-step maneuvering by two-side jets and sensor fault signal are shown as the square signal and the cosine-type signal in Fig. 3, respectively. Especially, for the cosine-type sensor fault, the target aims to deteriorate the estimation of relative velocity, yaw angular velocity and pitch angular velocity with a large oscillation effect.

In this simulation, the states of the missile guidance system and the corresponding estimated states are plotted in Figs. 4-6. From the results in Figs. 4-6, the Luenberger observer-based controller could successfully track the system states at  $t = 0.06s$ , i.e., the Luenberger observer completely estimates the missile guidance system from  $t = 0.06s$ . From  $t = 1s$ , the target begins to perform sudden side-step maneuvering. Since the proposed Luenberger observer-based controller can quickly estimate the actuator fault, the effect of actuator fault can be cancelled out by the proposed MO



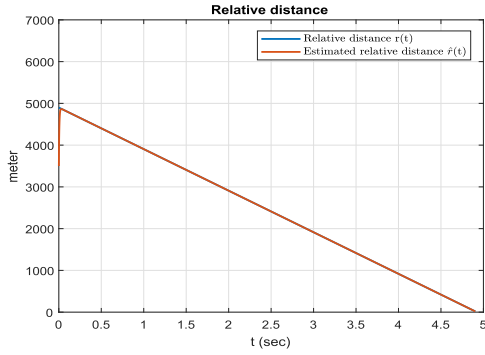


**FIGURE 4.** The relative distance and its estimation of missile guidance system by the proposed MO  $H_2/H_\infty$  observer-based fault-tolerant control under the effect of the square actuator fault signal and cosine-type sensor fault signal.

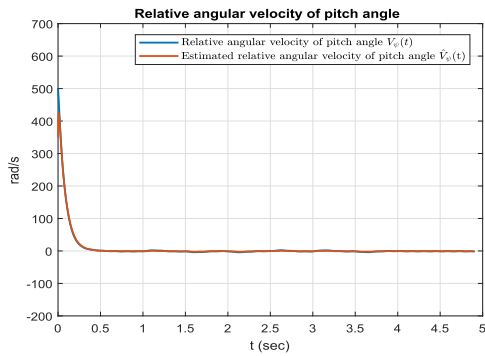


**FIGURE 5.** The relative pitch angular velocity and its estimation of missile guidance system by the proposed MO  $H_2/H_\infty$  observer-based fault-tolerant control under the effect of the square actuator fault signal and cosine-type sensor fault signal.

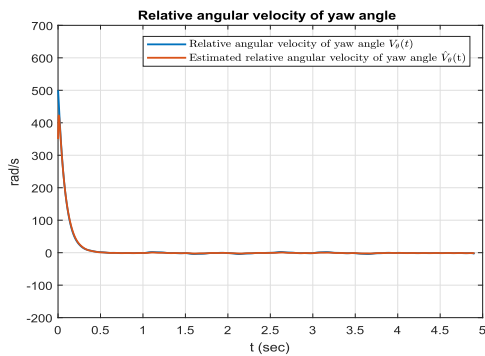


**FIGURE 6.** The relative yaw angular velocity and its estimation of missile guidance system by the proposed MO  $H_2/H_\infty$  observer-based fault-tolerant control under the effect of the square actuator fault signal and cosine-type sensor fault signal.

$H_2/H_\infty$  observer-based fault-tolerant controller, i.e., the actuator fault is cancelled by the estimated actuator fault. For the cosine-type sensor fault signal, Figs. 5-6 reveals the relative angular velocity of yaw angle and relative angular velocity of pitch angle are slightly fluctuate around the real states in the control process. By the proposed MO  $H_2/H_\infty$  observer-based fault-tolerant controller, the missile can successfully hit the target at  $t = 4.9s$  with the head-on condition, i.e., the relative

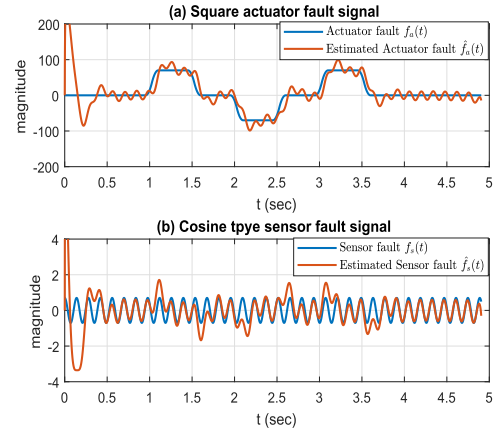


**FIGURE 7.** (a) The square actuator fault signal and its estimation. (b) the cosine-type sensor fault signal and its estimation.

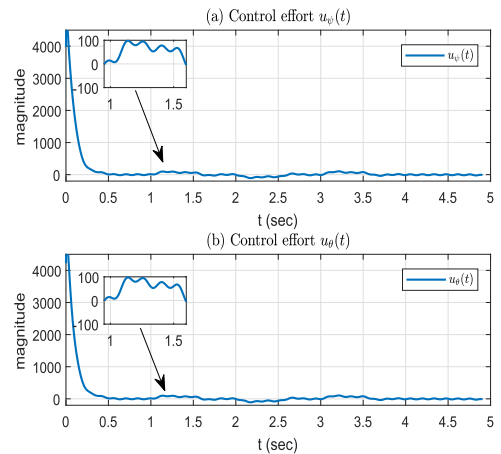


**FIGURE 8.** (a) The control signal of  $u_\psi(t)$ . (b) the control signal of  $u_\theta(t)$ . Once the actuator fault signal appear in the system, the control inputs will employ estimated actuator fault signal to eliminate the effect of real actuator fault signals.

distance, yaw angular velocity and pitch angular velocity of missile guidance system approach to 0 at  $t = 4.9s$ . Once the target is hit, the actuator and sensor fault signals vanished after  $t = 4.9s$ .

The simulation results in Fig. 7 shows the actuator and sensor fault and their estimation. In the beginning, due to the large estimation error (large initial condition) on the missile guidance system state, there have large but short estimated actuator and sensor fault signals. After that, the Luenberger observer can precisely estimate the actuator and sensor fault signals. The control strategies  $u_\psi(t)$  and  $u_\theta(t)$  are shown in Fig. 8 and it is seen that the proposed observer-based control strategies are effective to achieve the missile guidance task. Moreover, once the actuator fault signal is estimated, it can be seen that the control strategies will use estimated actuator fault signal to eliminate the real actuator fault signal. In general, due to the external disturbance, the actuator and sensor fault signal from the target, it is much difficult for the missile to achieve the head-on condition, i.e., the control

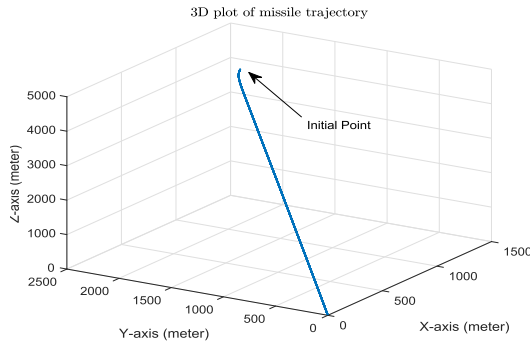


FIGURE 9. 3D graph of missile system. After a short transient state response, the missile can achieve the head-on condition to hit the target.

period is enlarged by the actuator and sensor fault signal. Nevertheless, by the proposed MO  $H_2/H_\infty$  observer-based fault-tolerant controller, the effect of external disturbance on the missile guidance system is greatly attenuated and the effect of actuator and sensor fault signal is eliminated. Hence, from the 3D graph in Fig. 9, the missile can maintain the head-on condition and successfully hit the target. The code file is included in [48] for performance validation.

Example 2: In this simulation example, the FTC design problem of balancing and swing-up of an inverted pendulum on a cart is considered. The pendulum motion can be explicitly expressed by the following fuzzy system with two IF-THEN rules [46]:

$$\begin{aligned} \dot{x}(t) &= \sum_{i=1}^2 h_i(x(t))(A_i x(t) + B_i u(t) \\ &\quad + B_{a,i} f_a(t) + B_{w,i} w(t)) \\ y(t) &= Cx(t) + n(t), \quad x(0) = [3 \ 1]^T \end{aligned} \quad (42)$$

where  $x(t) = [x_1(t) \ x_2(t)]^T \in \mathbb{R}^2$  denotes the state vector with the angle of pendulum  $x_1(t)$  (rad) and the corresponding angular velocity  $x_2(t)$  (rad/s),  $u(t)$  is the force (N) to the cart,  $f_a(t)$  is the actuator fault signal,  $w(t)$  is the external disturbance to the cart,  $y(t)$  represents the measurement output and  $n(t)$  is the measurement noise. The matrices in (42) are given as

$$\begin{aligned} A_1 &= \begin{bmatrix} 0 & 1 \\ \frac{g}{4l/3 - aml} & 0 \end{bmatrix}, \quad A_2 = \begin{bmatrix} 0 & 1 \\ \frac{2g}{\pi(4l/3 - aml\beta^2)} & 0 \end{bmatrix} \\ B_{a,1} = B_1 &= \begin{bmatrix} 0 & -\frac{g}{4l/3 - aml} \end{bmatrix}^T, \quad C = [1 \ 0] \\ B_{a,2} = B_2 &= \begin{bmatrix} 0 & -\frac{\alpha\beta}{4l/3 - aml\beta^2} \end{bmatrix}^T, \end{aligned}$$

with the gravity constant  $g = 9.8m/s^2$ , mass of the car  $M = 2kg$ , mass of the pendulum  $m = 2kg$ , half length of pendulum  $l = 0.5m$ , interpolation functions  $h_1(x_1(t)) = 1/(1 + \exp(x_1(t) + 0.5))$  and  $h_2(x_1(t)) = 1 - h_1(x_1(t))$  and  $a = 1/(M + m)$ .

To efficiently estimate the actuator fault signal  $f_a(t)$  in (42), the 3rd order smoothed signal model is chosen with the

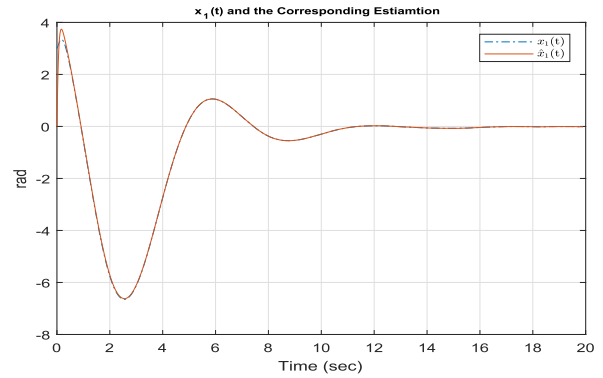


FIGURE 10. The trajectory of state  $x_1(t)$  and its estimation.

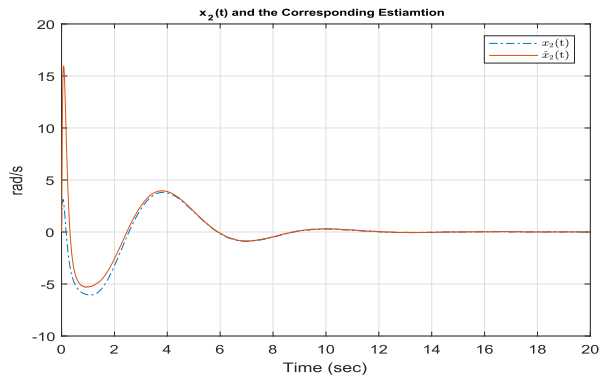


FIGURE 11. The trajectory of state  $x_2(t)$  and its estimation.

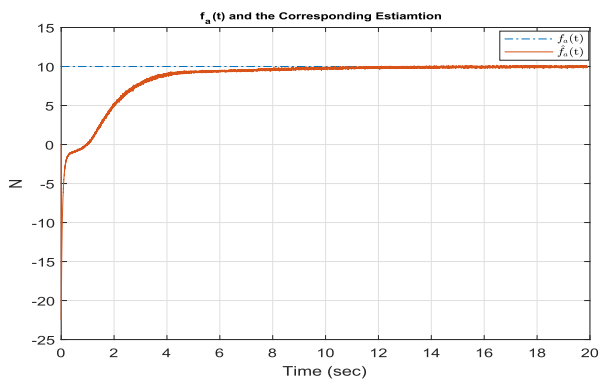


FIGURE 12. The fault signal  $f_a(t)$  and its estimation.

extrapolation coefficients  $\alpha_0 = 0.6$ ,  $\alpha_1 = 0.2$ ,  $\alpha_2 = 0.1$ , and  $\alpha_3 = 0.1$  of  $A_{f_a}$  in (5). Also, the 3rd order smoothed signal model for sensor fault signal is chosen with the extrapolation coefficients  $\beta_0 = 0.6$ ,  $\beta_1 = 0.2$ ,  $\beta_2 = 0.15$ , and  $\beta_3 = 0.05$  of  $A_{f_s}$  in (6). Since the pendulum system is free of sensor fault signal, the weighting matrix in (27) is chosen as:

$$\begin{aligned} \tilde{Q}_1 &= \text{diag}\{0_{8 \times 8}, I_2, I_4, 0_{4 \times 4}, I_2\} \\ \tilde{Q}_2 &= \text{diag}\{0_{8 \times 8}, 2I_2, I_4, 0_{4 \times 4}, 2I_2\} \\ \tilde{R}_2 &= 1 \end{aligned}$$

, i.e., the weightings of sensor fault estimation in  $\tilde{Q}_1$  and  $\tilde{Q}_2$  are zero, respectively. In this simulation example, the detailed parameters of reverse-MOEA are selected as: searching

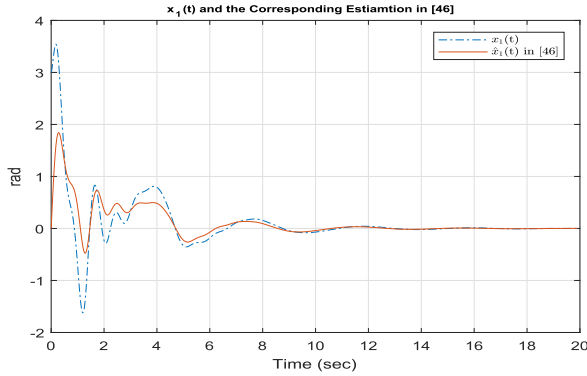


FIGURE 13. The trajectory of state  $x_1(t)$  and its estimation by the method in [46].

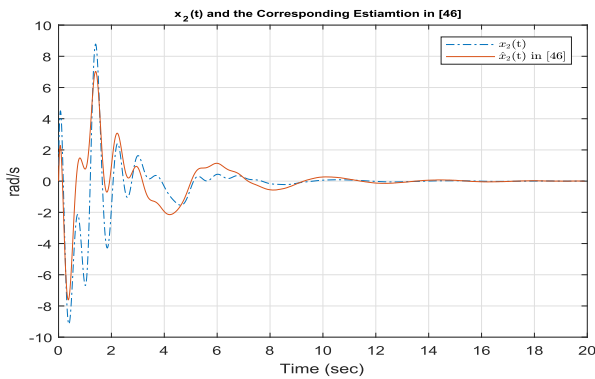


FIGURE 14. The trajectory of state  $x_2(t)$  and its estimation by the method in [46].

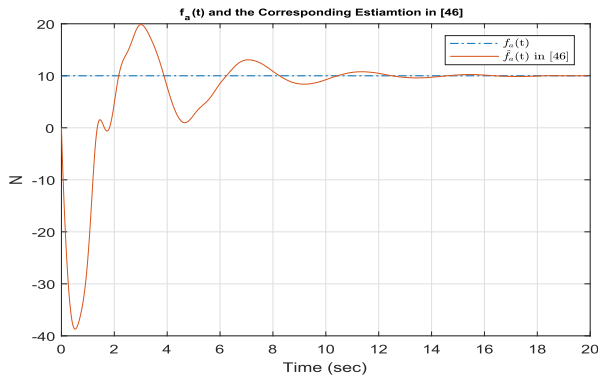


FIGURE 15. The fault signal  $f_a(t)$  and its estimation by the method in [46].

region  $R = [10.5, 50] \times [0.9, 10]$ , population number  $N_p = 120$ , iteration number  $N_i = 100$ , crossover rate  $C_r = 0.8$  and mutation rate  $C_m = 0.1$ . Then, by solving the MOP in (28), the optimal control performance  $(\alpha^*, \beta^*) = (23.21, 1.31)$  is selected and the corresponding design variables can refer to [47].

In this simulation, the external disturbance and the measurement noise are set as  $0.1N(0, 0.2)$  and  $0.1N(0, 0.2)$ , respectively. The actuator fault signal  $f_a(t) = 10$ , for 0s–20s, is set to represent unknown constant fault in actuator. The simulation results are shown in Figs. 10–15.

From Figs. 10–11, the pendulum system can be effectively stabilized to zero with a great disturbance attenuation level. Furthermore, since the actuator fault signal  $f_a(t)$  is precisely estimated in Fig. 12, its effect can be effectively eliminated by the proposed FTC design. The FTC design in [46] is carried out for the comparison with our design. From Figs. 13–14, it can be clearly seen that the state variables severely oscillate during the control process. On the other hand, from Fig. 15, the transient state response for fault estimation is large with some oscillation. As a result, due to the feedback of these imprecise fault signal estimation, the system may cause some undesired control performance. The code file is included in [48] for performance validation.

## VI. CONCLUSION

Based on the proposed dynamic smoothed signal model, a novel reverse-order MOEA was proposed to solve a complex multi-objective observer-based FTC of T-S fuzzy system, which could not be solved by the conventional MOEA due to large fuzzy control parameters and fuzzy observer parameters to be selected by evolution algorithm for multi-objective optimization. Through the proposed indirect suboptimal method, the multi-objective observer-based FTC design problem is reduced to an LMIs-constrained MOP, which could be efficiently solved by the proposed reverse-order MOEA with the help of LMI TOOLBOX in MATLAB via convex optimization algorithm such as interior point method. Finally, the proposed reverse-order MOEA is applied to efficiently solve the complex multi-objective  $H_2/H_\infty$  observer-based 3-D missile fault-tolerant guidance control problem with sensor and actuator faults, due to sudden cheating maneuvering jet and hostile interference. Also, the proposed method is applied to the FTC design for inverted pendulum system in comparison with state-of-the-art FTC method. In the future, the proposed reverse-order MOEA could be an efficient scheme to solve different MOPs control and estimation of complex T-S fuzzy system in both the application and research fields. Besides, along with the rapid development of internet of thing (IOT), the information can be quickly exchanged in the networked system via wireless communication technique to achieve more challenging tasks. Meanwhile, there may exist some malicious signals from the attackers who try to deteriorate the networked system and interfere the transmitted signal. Since the requirement of safety and reliability for networked system becomes an important issue, the proposed FTC method will be applied to the networked-based control system to achieve multi-objective optimal design with the consideration of malicious attack signals in the future.

## APPENDIX A PROOF OF THEOREM 1

By the rank test in [45], the  $i$ th augmented fuzzy system in (7) is observable if the following rank

condition holds:

$$\begin{aligned} & \text{rank} \begin{bmatrix} sI_{n+(k+1)(n_a+n_s)} - \bar{A}_i \\ C_i \end{bmatrix} \\ &= \text{rank} \begin{bmatrix} sI_{(k+1)n_a} - A_{f_a} & 0 & 0 \\ 0 & sI_{(k+1)n_s} - A_{f_s} & 0 \\ -B_{a,i}C_{f_a} & 0 & sI_n - A_i \\ 0 & D_iC_{f_s} & C_i \end{bmatrix} \\ &= n + n_a(k+1) + n_s(k+1), \quad \forall s \in \mathcal{S} \end{aligned} \quad (43)$$

where  $\mathcal{S}$  denotes the set of one-dimensional complex number. In the following, the proof is separated into two cases with (i)  $s \in \mathcal{S} \setminus (\text{eig}\{A_i\} \cup \text{eig}\{A_{f_s}\} \cup \text{eig}\{A_{f_a}\})$  and (ii)  $s \in \text{eig}\{A_i\} \cup \text{eig}\{A_{f_s}\} \cup \text{eig}\{A_{f_a}\}$ .

In the case (i), we immediately have following rank condition:

$$\begin{aligned} & \text{rank}[sI_{(k+1)n_a} - A_{f_a}] = n_a(k+1) \\ & \text{rank}[sI_{(k+1)n_s} - A_{f_s}] = n_s(k+1) \\ & \text{rank}[sI_n - A_i] = n \\ & \quad \forall s \in \mathcal{S} \setminus (\text{eig}\{A_i\} \cup \text{eig}\{A_{f_s}\} \cup \text{eig}\{A_{f_a}\}) \end{aligned} \quad (44)$$

As a result, by (44), (43) is satisfied for  $s \in \mathcal{S} \setminus (\text{eig}\{A_i\} \cup \text{eig}\{A_{f_s}\} \cup \text{eig}\{A_{f_a}\})$ , i.e.,

$$\begin{aligned} & \text{rank} \begin{bmatrix} sI_{(k+1)n_a} - A_{f_a} & 0 & 0 \\ 0 & sI_{(k+1)n_s} - A_{f_s} & 0 \\ -B_{a,i}C_{f_a} & 0 & sI_n - A_i \\ 0 & D_iC_{f_s} & C_i \end{bmatrix} \\ &= n + n_a(k+1) + n_s(k+1), \\ & \quad \forall s \in \mathcal{S} \setminus (\text{eig}\{A_i\} \cup \text{eig}\{A_{f_s}\} \cup \text{eig}\{A_{f_a}\}) \end{aligned} \quad (45)$$

In the case (ii), by the assumption in (9) that the eigenvalues of  $(A_i, A_{f_s}, A_{f_a})$  are mutually independent and (10), we can decouple the rank condition in (43) as the sum of three rank conditions

$$\begin{aligned} & \text{rank} \begin{bmatrix} sI_{(k+1)n_a} - A_{f_a} & 0 & 0 \\ 0 & sI_{(k+1)n_s} - A_{f_s} & 0 \\ -B_{a,i}C_{f_a} & 0 & sI_n - A_i \\ 0 & D_iC_{f_s} & C_i \end{bmatrix} \\ &= \text{rank} \begin{bmatrix} sI_{(k+1)n_a} - A_{f_a} \\ -B_{a,i}C_{f_a} \end{bmatrix} + \text{rank} \begin{bmatrix} sI_n - A_i \\ C_i \end{bmatrix} \\ & \quad + \text{rank} \begin{bmatrix} sI_{(k+1)n_s} - A_{f_s} \\ D_iC_{f_s} \end{bmatrix} \\ & \quad \forall s \in \text{eig}\{A_i\} \cup \text{eig}\{A_{f_s}\} \cup \text{eig}\{A_{f_a}\} \end{aligned} \quad (46)$$

By applying the rank conditions in (8), (11) and (12), the rank condition in (46) can be written as:

$$\begin{aligned} & \text{rank} \begin{bmatrix} sI_{(k+1)n_a} - A_{f_a} \\ -B_{a,i}C_{f_a} \end{bmatrix} + \text{rank} \begin{bmatrix} sI_{(k+1)n_s} - A_{f_s} \\ D_iC_{f_s} \end{bmatrix} \\ & \quad + \text{rank} \begin{bmatrix} sI_n - A_i \\ C_i \end{bmatrix} = n + n_a(k+1) + n_s(k+1) \\ & \quad \forall s \in \text{eig}\{A_i\} \cup \text{eig}\{A_{f_s}\} \cup \text{eig}\{A_{f_a}\} \end{aligned} \quad (47)$$

Thus, the observable condition for the  $i$ th augmented fuzzy system in (7) is guaranteed.

Q. E. D.

## APPENDIX B PROOF OF THEOREM 2

Consider the  $H_2$  observer-based fault-tolerant control in (20) and the Lyapunov function  $V(\tilde{x}(t)) = \tilde{x}^T(t)P\tilde{x}(t)$  with the case  $\bar{w}(t) = 0$  in (18), we have

$$\begin{aligned} & H_2(\{L_i, K_j\}_{i,j=1}^I) \\ &= \int_0^{t_f} \tilde{x}^T(t)\tilde{Q}_2\tilde{x}(t) + u^T(t)\tilde{R}_2u(t)dt \\ &= \int_0^{t_f} \tilde{x}^T(t)\tilde{Q}_2\tilde{x}(t) + u^T(t)\tilde{R}_2u(t)dt + dV(\tilde{x}(t)) \\ & \quad + \tilde{x}^T(0)P\tilde{x}(0) - \tilde{x}^T(t_f)P\tilde{x}(t_f) \\ &= \sum_{i=1}^I \sum_{j=1}^I h_i(z(t))h_j(z(t)) \int_0^{t_f} \tilde{x}^T(t) \left( P\tilde{A}_{ij} + \tilde{A}_{ij}^T P + \tilde{Q}_2 \right. \\ & \quad \left. + \tilde{K}_j^T \tilde{R}_2 \tilde{K}_j \right) \tilde{x}(t) dt + \tilde{x}^T(0)P\tilde{x}(0) - \tilde{x}^T(t_f)P\tilde{x}(t_f), \end{aligned} \quad (48)$$

where  $\tilde{K}_j = [K_j, -K_j]$  with the positive-definite matrix  $P > 0$ . Clearly, if the matrix inequality constraints in (24) and (25) hold, we immediately have the following results:

$$H_2(\{K_i, L_j\}_{i,j=1}^I) \leq \alpha,$$

which satisfies the optimal  $H_2$  constraint in (22).

On the other hand, for the robust  $H_\infty$  FTC performance in (19), we have

$$\begin{aligned} & \int_0^{t_f} [\tilde{x}^T(t)\tilde{Q}_1\tilde{x}(t)]dt \\ &= \int_0^{t_f} ([\tilde{x}^T(t)\tilde{Q}_1\tilde{x}(t)]dt + dV(\tilde{x}(t))) \\ & \quad + \tilde{x}^T(0)P\tilde{x}(0) - \tilde{x}^T(t_f)P\tilde{x}(t_f) \\ &= \sum_{j,i=1}^I h_i(t)h_j(t) \int_0^{t_f} [\tilde{x}^T(t)(P\tilde{A}_{ij} + \tilde{A}_{ij}^T P + \tilde{Q}_1)\tilde{x}(t) \\ & \quad + \tilde{x}^T(t)P\tilde{D}_{ij}\tilde{w}(t) + \tilde{w}^T(t)\tilde{D}_{ij}^T P\tilde{x}(t)]dt \\ & \quad + \tilde{x}^T(0)P\tilde{x}(0) - \tilde{x}^T(t_f)P\tilde{x}(t_f). \end{aligned} \quad (49)$$

By utilizing Lemma 1 with some  $\beta > 0$ , we have:

$$\begin{aligned} & \tilde{x}^T(t)P\tilde{D}_{ij}\tilde{w}(t) + \tilde{w}^T(t)\tilde{D}_{ij}^T P\tilde{x}(t) \\ & \leq \frac{1}{\beta} \tilde{x}^T(t)P\tilde{D}_{ij}\tilde{D}_{ij}^T P\tilde{x}(t) + \beta \tilde{w}^T(t)\tilde{w}(t), \\ & \quad \forall i, j = 1, \dots, I. \end{aligned} \quad (50)$$

Substituting (50) into (49), we have:

$$\begin{aligned} & \int_0^{t_f} \tilde{x}^T(t)\tilde{Q}_1\tilde{x}(t)dt \\ & \leq \sum_{j,i=1}^I \int_0^{t_f} [\tilde{x}^T(t)(P\tilde{A}_{ij} + \tilde{A}_{ij}^T P + \tilde{Q}_1 \\ & \quad + \frac{1}{\beta} P\tilde{D}_{ij}\tilde{D}_{ij}^T P)\tilde{x}(t) + \beta \tilde{w}^T(t)\tilde{w}(t)]dt \\ & \quad + \tilde{x}^T(0)P\tilde{x}(0). \end{aligned} \quad (51)$$



If the matrix constraints (26) hold, we immediately have:

$$\begin{aligned} & \int_0^{t_f} \tilde{x}^T(t) \tilde{Q}_1 \tilde{x}(t) dt \\ & \leq \int_0^{t_f} \beta \tilde{w}^T(t) \tilde{w}(t) dt + \tilde{x}^T(0) P \tilde{x}(0) \\ & \quad \forall \tilde{w}(t) \in \mathcal{L}_2(\mathbb{R}^+; \mathbb{R}^{n_w}), \end{aligned} \quad (52)$$

and  $H_\infty(\{L_i, K_j\}_{i,j=1}^I) \leq \beta$ . Hence, the MOP in (22) is transformed to the matrix inequalities-constrained MOP in (23).

Q.E.D

**APPENDIX C  
PROOF OF THEOREM 3**

By using Schur complement [41], the inequalities in (24) are equivalent to:

$$\begin{bmatrix} P\tilde{A}_{ij} + \tilde{A}_{ij}^T P + \tilde{Q}_2 & \tilde{K}_j^T \\ * & -\tilde{R}_2^{-1} \end{bmatrix} \leq 0 \quad \text{for } i, j = 1, \dots, I \quad (53)$$

From (16) and (17), (53) can be rewritten as:

$$\begin{bmatrix} \Delta_{2,1} & -P_1 \tilde{B}_{u,i} K_j & K_j^T \\ * & \Delta_{2,2} & -K_j^T \\ * & * & -\tilde{R}_2^{-1} \end{bmatrix} \leq 0 \quad \text{for } i, j = 1, \dots, I. \quad (54)$$

where  $\Delta_{2,1} = P_1 \tilde{A}_i + P_1 \tilde{B}_{u,i} K_j + \tilde{A}_i^T P_1 + K_j^T \tilde{B}_{u,i}^T P_1 + \tilde{Q}_{2,\bar{x}}$ ,  $\Delta_{2,2} = P_2 \tilde{A}_i - P_2 L_i \tilde{C}_j + \tilde{A}_i^T P_2 - \tilde{C}_j^T L_i^T P_2 + \tilde{Q}_{2,e}$ .

By multiplying  $\text{diag}\{W_1, I, I\}$  to both side of (54) with  $W_1 = P_1^{-1}$ , we have:

$$\begin{bmatrix} \Delta'_{2,1} & -\tilde{B}_{u,i} K_j & W_1 K_j^T \\ * & \Delta'_{2,2} & -K_j^T \\ * & * & -\tilde{R}_2^{-1} \end{bmatrix} \leq 0, \quad \text{for } i, j = 1, \dots, I \quad (55)$$

where  $\Delta'_{2,1} = \tilde{A}_i W_1 + \tilde{B}_{u,i} K_j W_1 + W_1 \tilde{A}_i^T + W_1 K_j^T \tilde{B}_{u,i}^T + W_1 \tilde{Q}_{2,\bar{x}} W_1$ ,  $\Delta'_{2,2} = P_2 \tilde{A}_i - P_2 L_i \tilde{C}_j + \tilde{A}_i^T P_2 - \tilde{C}_j^T L_i^T P_2 + \tilde{Q}_{2,e}$ . By using Schur complement again, (55) can be rewritten as:

$$\begin{bmatrix} \Delta''_{2,1} & -\tilde{B}_{u,i} K_j & W_1 K_j^T & W_1 (\tilde{Q}_{2,\bar{x}})^{\frac{1}{2}} \\ * & \Delta''_{2,2} & -K_j^T & 0 \\ * & * & -\tilde{R}_2^{-1} & 0 \\ * & * & * & -I \end{bmatrix} \leq 0, \quad \text{for } i, j = 1, \dots, I \quad (56)$$

where  $\Delta''_{2,1} = \tilde{A}_i W_1 + \tilde{B}_{u,i} K_j W_1 + W_1 \tilde{A}_i^T + W_1 K_j^T \tilde{B}_{u,i}^T$ ,  $\Delta''_{2,2} = P_2 \tilde{A}_i - P_2 L_i \tilde{C}_j + \tilde{A}_i^T P_2 - \tilde{C}_j^T L_i^T P_2 + \tilde{Q}_{2,e}$ .

For the constraint in (25), by using Schur complement [41], the inequality in (25) can be transformed to the matrix inequality as follows:

$$\begin{aligned} & \tilde{x}^T(0) P \tilde{x}(0) \leq \alpha, \\ & \implies e^T(0) P_2 e(0) + \tilde{x}^T(0) P_1 \tilde{x}(0) - \alpha \leq 0, \\ & \implies \begin{bmatrix} e^T(0) P_2 e(0) - \alpha & \tilde{x}^T(0) \\ \tilde{x}(0) & -W_1 \end{bmatrix} \leq 0. \end{aligned}$$

At last, we consider the  $H_\infty$  matrix constraints in (26). By using Schur complement [41], the inequalities in (26) can be rewritten as:

$$\begin{bmatrix} P\tilde{A}_{ij} + \tilde{A}_{ij}^T P + \tilde{Q}_1 & P\tilde{D}_{ij} \\ * & -\beta I \end{bmatrix} \leq 0 \quad \text{for } i, j = 1, \dots, I. \quad (57)$$

From (16) and (18), (57) can be rewritten as:

$$\begin{bmatrix} \Delta_{\infty,1} & -P_1 \tilde{B}_{u,i} K_j & P_1 \tilde{B}_{w,i} \\ * & \Delta_{\infty,2} & P_2 \tilde{B}_{w,i} - P_2 L_i \tilde{D}_j \\ * & * & -\beta I \end{bmatrix} \leq 0 \quad \text{for } i, j = 1, \dots, I, \quad (58)$$

where  $\Delta_{\infty,1} = P_1 \tilde{A}_i + P_1 \tilde{B}_{u,i} K_j + \tilde{A}_i^T P_1 + K_j^T \tilde{B}_{u,i}^T P_1 + \tilde{Q}_{1,\bar{x}}$ ,  $\Delta_{\infty,2} = P_2 \tilde{A}_i - P_2 L_i \tilde{C}_j + \tilde{A}_i^T P_2 - \tilde{C}_j^T L_i^T P_2 + \tilde{Q}_{1,e}$ .

By multiplying  $\text{diag}\{W_1, I, I\}$  to both sides of (58) with  $W_1 = P_1^{-1}$ , we have

$$\begin{bmatrix} \Delta'_{\infty,1} & -\tilde{B}_{u,i} K_j & \tilde{B}_{w,i} \\ * & \Delta'_{\infty,2} & P_2 \tilde{B}_{w,i} - P_2 L_i \tilde{D}_j \\ * & * & -\beta I \end{bmatrix} \leq 0 \quad \text{for } i, j = 1, \dots, I, \quad (59)$$

where  $\Delta'_{\infty,1} = \tilde{A}_i W_1 + \tilde{B}_{u,i} K_j W_1 + W_1 \tilde{A}_i^T + W_1 K_j^T \tilde{B}_{u,i}^T + W_1 \tilde{Q}_{1,\bar{x}} W_1$ ,  $\Delta'_{\infty,2} = P_2 \tilde{A}_i - P_2 L_i \tilde{C}_j + \tilde{A}_i^T P_2 - \tilde{C}_j^T L_i^T P_2 + \tilde{Q}_{1,e}$ . By applying Schur complement again, (59) can be rewritten as:

$$\begin{bmatrix} \Delta''_{\infty,1} & -\tilde{B}_{u,i} K_j & \tilde{B}_{w,i} & W_1 (\tilde{Q}_{1,\bar{x}})^{\frac{1}{2}} \\ * & \Delta''_{\infty,2} & P_2 \tilde{B}_{w,i} - P_2 L_i \tilde{D}_j & 0 \\ * & * & -\beta I & 0 \\ * & * & * & -I \end{bmatrix} \leq 0 \quad \text{for } i, j = 1, \dots, I \quad (60)$$

where  $\Delta''_{\infty,1} = \tilde{A}_i W_1 + \tilde{B}_{u,i} K_j W_1 + W_1 \tilde{A}_i^T + W_1 K_j^T \tilde{B}_{u,i}^T$ ,  $\Delta''_{\infty,2} = P_2 \tilde{A}_i - P_2 L_i \tilde{C}_j + \tilde{A}_i^T P_2 - \tilde{C}_j^T L_i^T P_2 + \tilde{Q}_{1,e}$ . It is obvious that the BMIs in (60) are the constraints in (31).

Q. E. D.

**REFERENCES**

- [1] R. J. Patton, "Fault-tolerant control systems: The 1997 situation," in *Proc. IFAC Symp. Safeprocess*, 1997, pp. 1033-1054.
- [2] M. Blanke, R. Izadi-Zamanabadi, S. A. Bøgh, and C. P. Lunau, "Fault-tolerant control systems—A holistic view," *Control Eng. Pract.*, vol. 5, no. 5, pp. 693-702, May 1997.
- [3] A. Shui, W. Chen, P. Zhang, S. Hu, and X. Huang, "Review of fault diagnosis in control systems," in *Proc. IEEE 21st Chin. Control Decis. Conf.*, New York, NY, USA, Jun. 2009, pp. 5324-5329.
- [4] H. Lee and Y. Kim, "Fault-tolerant control scheme for satellite attitude control system," *IET Control Theory Appl.*, vol. 4, no. 8, pp. 1436-1450, Aug. 2010.
- [5] S. Wang and D. Dong, "Fault-tolerant control of linear quantum stochastic systems," *IEEE Trans. Autom. Control*, vol. 62, no. 6, pp. 2929-2935, Jun. 2017.
- [6] S. Kawahata, M. Deng, and S. Wakitani, "Operator theory based nonlinear fault tolerance control for MIMO microreactor," in *Proc. UKACC 11th Int. Conf. Control (CONTROL)*, Belfast, U.K., Aug. 2016, pp. 1-6.
- [7] F. Chen, J. Niu, and G. Jiang, "Nonlinear fault-tolerant control for hypersonic flight vehicle with multi-sensor faults," *IEEE Access*, vol. 6, pp. 25427-25436, 2018.

- [8] N. Li, X. Y. Luo, K. Xu, and X. P. Guan, "Robust  $H_\infty$  fault-tolerant control for nonlinear time-delay systems against actuator fault," in *Proc. 31st Chin. Control Conf.*, Hefei, China, Jul. 2012, pp. 5265–5270.
- [9] T. Takagi and M. Sugeno, "Fuzzy identification of systems and its applications to modeling and control," *IEEE Trans. Syst., Man, Cybern.*, vol. SMC-15, no. 1, pp. 116–132, Jan. 1985.
- [10] K. Tanaka and H. O. Wang, *Fuzzy Control Systems Design and Analysis*. Hoboken, NJ, USA: Wiley, 2001.
- [11] D. Zhang, Q.-L. Han, and X. Jia, "Network-based output tracking control for a class of T-S fuzzy systems that can not be stabilized by non-delayed output feedback controllers," *IEEE Trans. Cybern.*, vol. 45, no. 8, pp. 1511–1524, Aug. 2015.
- [12] D. Zhang, Q.-L. Han, and X. Jia, "Network-based output tracking control for T-S fuzzy systems using an event-triggered communication scheme," *Fuzzy Sets Syst.*, vol. 273, pp. 26–48, Aug. 2015.
- [13] E.-H. Guechi, J. Lauber, M. Dambrine, G. Klančar, and S. Blažič, "PDC control design for non-holonomic wheeled mobile robots with delayed outputs," *J. Intell. Robotic Syst.*, vol. 60, nos. 3–4, pp. 395–414, Apr. 2010.
- [14] R.-E. Precup and M. L. Tomescu, "Stable fuzzy logic control of a general class of chaotic systems," *Neural Comput. Appl.*, vol. 26, no. 3, pp. 541–550, Jun. 2014.
- [15] Y.-X. Li and G.-H. Yang, "Fuzzy adaptive output feedback fault-tolerant tracking control of a class of uncertain nonlinear systems with nonaffine nonlinear faults," *IEEE Trans. Fuzzy Syst.*, vol. 24, no. 1, pp. 223–234, Feb. 2016.
- [16] P. Li and G. Yang, "Backstepping adaptive fuzzy control of uncertain nonlinear systems against actuator faults," *J. Control Theory Appl.*, vol. 7, no. 3, pp. 248–256, Aug. 2009.
- [17] X. Su, F. Xia, L. Wu, and C. L. P. Chen, "Event-triggered fault detector and controller coordinated design of fuzzy systems," *IEEE Trans. Fuzzy Syst.*, vol. 26, no. 4, pp. 2004–2016, Aug. 2018.
- [18] Y. Li, K. Sun, and S. Tong, "Observer-based adaptive fuzzy fault-tolerant optimal control for SISO nonlinear systems," *IEEE Trans. Cybern.*, vol. 49, no. 2, pp. 649–661, Feb. 2019.
- [19] Z. Wang, L. Liu, Y. Wu, and H. Zhang, "Optimal fault-tolerant control for discrete-time nonlinear strict-feedback systems based on adaptive critic design," *IEEE Trans. Neural Netw. Learn. Syst.*, vol. 29, no. 6, pp. 2179–2191, Jun. 2018.
- [20] S. K. Kommuri, S. B. Lee, and K. C. Veluvolu, "Robust sensors-fault-tolerance with sliding mode estimation and control for PMSM drives," *IEEE/ASME Trans. Mechatronics*, vol. 23, no. 1, pp. 17–28, Feb. 2018.
- [21] E. Kamal, A. Aitouche, R. Ghorbani, and M. Bayart, "Robust fuzzy fault-tolerant control of wind energy conversion systems subject to sensor faults," *IEEE Trans. Sustain. Energy*, vol. 3, no. 2, pp. 231–241, Apr. 2012.
- [22] B. S. Chen, C. S. Tseng, and H. J. Uang, "Mixed  $H_2/H_\infty$  fuzzy output feedback control design for nonlinear dynamic systems: An LMI approach," *IEEE Trans. Fuzzy Syst.*, vol. 8, no. 3, pp. 249–265, Jun. 2000.
- [23] K. Zhou, K. Glover, B. Bodenheimer, and J. Doyle, "Mixed  $H_2/H_\infty$  performance objectives I: Robust performance analysis," *IEEE Trans. Autom. Control*, vol. 39, pp. 1564–1574, Aug. 1994.
- [24] C.-F. Wu, B.-S. Chen, and W. Zhang, "Multiobjective investment policy for a nonlinear stochastic financial system: A fuzzy approach," *IEEE Trans. Fuzzy Syst.*, vol. 25, no. 2, pp. 460–474, Apr. 2017.
- [25] B.-S. Chen and S.-J. Ho, "Multiobjective tracking control design of T-S fuzzy systems: Fuzzy Pareto optimal approach," *Fuzzy Sets Syst.*, vol. 290, pp. 39–55, May 2016.
- [26] Y. Lin, T. Zhang, and W. Zhang, "Pareto-based guaranteed cost control of the uncertain mean-field stochastic systems in infinite horizon," *Automatica*, vol. 92, pp. 197–209, Jun. 2018.
- [27] K. Li, R. Chen, G. Min, and X. Yao, "Integration of preferences in decomposition multiobjective optimization," *IEEE Trans. Cybern.*, vol. 48, no. 12, pp. 3359–3370, Dec. 2018.
- [28] W.-Y. Chiu, B.-S. Chen, and H. V. Poor, "A multiobjective approach for source estimation in fuzzy networked systems," *IEEE Trans. Circuits Syst. I, Reg. Papers*, vol. 60, no. 7, pp. 1890–1900, Jul. 2013.
- [29] C.-S. Tseng and B.-S. Chen, "Multiobjective PID control design in uncertain robotic systems using neural network elimination scheme," *IEEE Trans. Syst., Man, Cybern. A, Syst. Humans*, vol. 31, no. 6, pp. 632–644, Nov. 2001.
- [30] G. P. Liu, J. B. Yang, and J. F. Whidborne, *Multiobjective Optimisation and Control*. London, U.K.: Research Studies Press, 2003.
- [31] X. S. Yang, *Nature-Inspired Optimization Algorithms*, 1st ed. Amsterdam, The Netherlands: Elsevier, Mar. 2014.
- [32] H. Zapata, N. Perozo, W. Angulo, and J. Contreras, "A hybrid swarm algorithm for collective construction of 3D structures," *Int. J. Artif. Intell.*, vol. 18, no. 1, pp. 1–18, Feb. 2020.
- [33] R. E. Precup and R. C. David, *Nature-Inspired Optimization Algorithms for Fuzzy Controlled Servo Systems*. London, U.K.: Butterworth, 2019.
- [34] K. Deb, *Multi-Objective Optimization Using Evolutionary Algorithms*. New York, NY, USA: Wiley, 2001.
- [35] K. Deb, A. Pratap, S. Agarwal, and T. Meyarivan, "A fast and elitist multiobjective genetic algorithm: NSGA-II," *IEEE Trans. Evol. Comput.*, vol. 6, no. 2, pp. 182–197, Apr. 2002.
- [36] A. Abraham and R. Goldberg, *Evolutionary Multiobjective Optimization: Theoretical Advances and Applications*. London, U.K.: Springer-Verlag, 2005.
- [37] B.-S. Chen and M.-Y. Lee, "Noncooperative and cooperative strategy designs for nonlinear stochastic jump diffusion systems with external disturbance: T-S fuzzy approach," *IEEE Trans. Fuzzy Syst.*, vol. 28, no. 10, pp. 2437–2451, Oct. 2020.
- [38] C.-F. Wu, B.-S. Chen, and W. Zhang, "Multiobjective  $H_2/H_\infty$  control design of the nonlinear mean-field stochastic jump-diffusion systems via fuzzy approach," *IEEE Trans. Fuzzy Syst.*, vol. 27, no. 4, pp. 686–700, Apr. 2019.
- [39] R. S. Varga, "Extrapolation methods: Theory and practice," *Numer. Algorithms*, vol. 4, no. 2, p. 305, Jan. 1993.
- [40] J. D. Stefanovski, "Fault tolerant control of descriptor systems with disturbances," *IEEE Trans. Autom. Control*, vol. 64, no. 3, pp. 976–988, Mar. 2019.
- [41] S. Boyd, L. E. Ghaoui, E. Feron, and V. Balakrishnan, *Linear Matrix Inequalities in System and Control Theory*. Philadelphia, PA, USA: SIAM, 1994.
- [42] C. F. Lin, *Modern Navigation, Guidance, and Control Processing*. Upper Saddle River, NJ, USA: Prentice-Hall, 1991.
- [43] N. F. Palumbo, R. A. Blauwkamp, and J. M. Lloyd, "Basic principles of homing guidance," *Johns Hopkins APL Tech. Dig.*, vol. 29, no. 1, pp. 25–41, Jan. 2010.
- [44] B.-S. Chen, Y.-Y. Chen, and C.-L. Lin, "Nonlinear fuzzy  $H_\infty$  guidance law with saturation of actuators against maneuvering targets," *IEEE Trans. Control Syst. Technol.*, vol. 10, no. 6, pp. 769–779, Nov. 2002.
- [45] S. H. Zak, *Systems and Control*. Oxford, U.K.: Oxford Univ. Press, 2003.
- [46] S.-J. Huang and G.-H. Yang, "Fault tolerant controller design for T-S fuzzy systems with time-varying delay and actuator faults: A K-step fault-estimation approach," *IEEE Trans. Fuzzy Syst.*, vol. 22, no. 6, pp. 1526–1540, Dec. 2014.
- [47] B. S. Chen, M. Y. Lee, W. Y. Chen, and W. H. Chang, *Supplementary Materials*. HsinChu, Taiwan. Accessed: Dec. 24, 2020. [Online]. Available: <https://www.dropbox.com/s/legwxkyozsiomvof/Silumation%20Parameters.pdf?dl=0>
- [48] B. S. Chen, M. Y. Lee, W. Y. Chen, and W. H. Chang, *Supplementary Materials*. HsinChu, Taiwan. Accessed: Dec. 24, 2020. [Online]. Available: <https://www.dropbox.com/s/dq8sc9gp8v17swf/code.rar?dl=0>



**BOR-SEN CHEN** (Life Fellow, IEEE) received the B.S. degree in electrical engineering from the Tatung Institute of Technology, Taipei, Taiwan, in 1970, the M.S. degree in geophysics from National Central University, Chungli, Taiwan, in 1973, and the Ph.D. degree in electrical engineering from the University of Southern California, Los Angeles, CA, USA, in 1982. He was a Lecturer, an Associate Professor, and a Professor with the Tatung Institute of Technology, from 1973 to 1987. He is currently the Tsing Hua Distinguished Chair Professor of electrical engineering and computer science with National Tsing Hua University, Hsinchu, Taiwan. His current research interests include control engineering, signal processing, and systems biology. He has received the Distinguished Research Award from the National Science Council of Taiwan four times. He is also the National Chair Professor of the Ministry of Education of Taiwan.



**MIN-YEN LEE** received the B.S. degree in bio-industrial mechatronics engineering from National Chung Hsing University, Taichung, Taiwan, in 2014. He is currently pursuing the Ph.D. degree with the Department of Electrical Engineering, National Tsing Hua University, Hsinchu, Taiwan. His current research interests include robust control, fuzzy control, and nonlinear stochastic systems.



**WEI-YU CHEN** received the B.S. degree from the Department of Electrical Engineering, National Dong Hwa University, Hualien, Taiwan, in 2014, and the M.S. degree from the Department of Electrical Engineering, National Tsing Hua University, Hsinchu, Taiwan, in 2016. He is currently a Research Assistant with the Research Center for Information Technology Innovation (CITI), Academia Sinica, Taipei, Taiwan. His current research interests include mobile edge computing, large intelligent surface (LIS), simultaneous wireless information and power transfer (SWIPT), and next-generation wireless communication systems.



**WEIHAI ZHANG** (Senior Member, IEEE) received the M.S. degree in probability theory and mathematical statistics and the Ph.D. degree in operations research and cybernetics from Hangzhou University (currently Zhejiang University), Hangzhou, China, in 1994 and 1998, respectively. He is currently a Professor with the Shandong University of Science and Technology. He is also a Taishan Scholar of Shandong Province of China. He has published more than 110 peer-reviewed journal articles and one monograph *Stochastic H<sub>2</sub>/H<sub>∞</sub> Infinity Control: A Nash Game Approach* (Boca Raton, FL, USA: CRC Press, 2017). His research interests include linear and nonlinear stochastic optimal control, mean-field systems, robust H infinity control, stochastic stability and stabilization, multi-objective optimization, and fuzzy adaptive control. He is also a member of the Technical Committee on Control Theory of Chinese Association of Automation. He received the Second Prize of the Ministry of Education of the People's Republic of China twice. He serves as an Associate Editor for the *Asian Journal of Control* and the *Journal of the Franklin Institute*.

• • •